Yu, H. S. & Houlsby, G. T. (1991). *Géotechnique* **41**, No. 2, 173–183

Finite cavity expansion in dilatant soils: loading analysis

H. S. YU* and G. T. HOULSBY†

An analysis of the quasi-static expansion of a cylindrical or spherical cavity in an infinite dilatant elastic–plastic soil is presented. Closed form solutions for the stress and displacement fields in the soil during the expansion of the cavity are given. The soil is modelled as linear elastic–perfectly plastic, using a non-associated Mohr–Coulomb yield criterion. An explicit solution for the pressure–expansion relationship is obtained with no restriction on the magnitude of the deformation. It is found, in particular, that the radius of the cavity increases indefinitely as the cavity pressure approaches a finite limiting value. This limiting pressure can be determined analytically with the help of a single expansion of an infinite series. The novelty of the new solution lies in the introduction of dilation to the analysis of large strain expansion. Examples of the implications of the new analysis in geotechnical engineering are discussed.

KEYWORDS: analysis; elasticity; friction; plasticity; strains; stress analysis.

L'article présente une analyse de l'expansion quasi-statique d'une cavité cylindrique ou sphérique dans un sol élastoplastique de dilatance infinie. Des solutions de forme fermée sont présentées pour les champs de contrainte et de déplacement dans le sol au cours de l'expansion de la cavité. Le sol est modelisé comme élastique linéaire/parfaitement plastique, en employant un critère de rendement non-associé type Mohr–Coulomb. Une solution explicite pour la relation pression/expansion est obtenue sans restriction sur la valeur de la déformation. On trouve plus particulièrement que le rayon de la cavité augmente de façon indéfinie au fur et à mesure que la pression de cavité s'approche d'une valeur limite finie. Cette pression limite peut se déterminer par analyse à l'aide d'une seule expansion d'une série infinie. La nouveauté de la nouvelle solution réside dans l'inclusion de la dilatation dans l'analyse des expansions de déformation de valeur élevée. On examine des exemples des implications de la nouvelle analyse pour la construction géotechnique.

INTRODUCTION

Cavity expansion theory has several applications in soil mechanics, principally in the areas of interpretation of in situ tests (both the cone penetrometer and the pressuremeter) and also in the prediction of the behaviour of piles. Many papers on this topic have been published and the principal ones are briefly reviewed here. The purpose of this Paper is to present a large-strain analysis of cavity expansion in dilatant soils. This problem has important applications to the understanding of in situ tests and piling in dense granular materials. Large-strain analysis is essential if some features of soil behaviour are to be included, particularly the existence of a limit pressure. The combination of large-strain theory with the dilatant material model means that some of the analysis is necessarily rather complex mathematically. The end result, however, is a fairly straightforward procedure which can be used to construct the pressure–expansion relationship. A slight simplification is achieved by using small-strain theory in the elastically deforming zone, an approximation which is justified for all realistic soil properties.

Discussion on this Paper closes 4 October 1991; for further details see p. ii.

* University of Newcastle, NSW 2308, Australia, formerly Department of Engineering Science, Oxford University, OX1 3PJ, UK.

† Department of Engineering Science, Oxford University.

Previous work on cavity expansion

Cavity expansion theory was first developed for application to metal indentation problems (Bishop *et al.*, 1945; Hill, 1950). The application of cavity expansion theory to geotechnical problems came later (e.g. Gibson & Anderson, 1961) and has been progressively refined over the past two decades. The analysis of a cylindrical cavity has been applied to practical problems such as the interpretation of pressuremeter tests (Gibson & Anderson, 1961; Palmer, 1972; Hughes *et al.*, 1977; Houlsby *et al.*, 1986; Houlsby & Withers, 1988) allowing the pressure–expansion curve obtained in a pressuremeter test to be interpreted directly in terms of soil properties. A detailed study of the application of cylindrical cavity expansion in modelling the installation of driven piles was given by Randolph *et al.* (1979). The effect of longitudinal shaft friction in a cylindrical expanding cavity, which is important for application to pile bearing capacity analysis, has been considered by Sagaseta (1984). It should be noted that all these analytical studies are either large-strain analyses of incompressible soils or small-strain analyses of dilatant soils. The large-strain cavity expansion problem in dilatant soil has, therefore, usually been solved using a finite element method (Carter & Yeung, 1985; Yu & Houlsby, 1990). However, it is accepted that severe numerical difficulties arise when using the finite element method to analyse constrained problems (e.g. those involving incompressible or dilatant solids). Hence care must be taken when using the conventional finite element approach to model elastic–plastic soil behaviour. A study of the numerical difficulties in using the conventional finite element method to model elastic–plastic deformation involving incompressibility and dilatancy is given by Yu (1990).

As far as the spherical cavity problem is concerned, some solutions have been obtained for cavities in various types of materials. Hill (1950) gave a general solution of the finite expansion of the spherical cavity in a Tresca material. Later Chadwick (1959) presented a more comprehensive solution for the expansion of a spherical cavity in an elastic–plastic material obeying the associated Mohr–Coulomb flow rule. The closed form limit pressure for the special case of a purely cohesive incompressible material was also presented in the same paper. Vesic (1972) extended the analysis to compressible soils by allowing for the possibility that the volumetric strain is not zero, and presented an approximate solution for limit pressure for spherical cavity expansion. He applied this solution to the determination of bearing capacity factors for deep foundations.

More recently, Carter *et al.* (1986) presented an analytical solution for limit pressures for cavity expansion in a non-associated Mohr–Coulomb material, by assuming that a steady state deformation mode is approached at very large deformations. It is believed that there are certain unjustified approximations made in the subsequent analysis and that the limit pressure solution presented in their paper can only be treated as approximate.

The important role of the elastic deformations in the plastic zone for the cavity expansion problem is emphasized by Bigoni & Laudiero (1989), who solved the cavity expansion problem partly analytically and partly using numerical (Gaussian) integration. In their paper, a similar approach to Chadwick's was used and the non-associated Mohr–Coulomb criterion was adopted. In the cylindrical case they assumed that the longitudinal normal stress was equal to the mean of the other two principal stresses. However, this assumption means that the flow rule which determines the plastic strains in the axial direction is violated.

In this Paper, a unified analytical solution is presented for the expansion of both cylindrical and spherical cavities in dilatant elastic–plastic soils using the Mohr–Coulomb yield criterion with a non-associated flow rule. For the case of cylindrical cavity expansion, the axial or vertical stress is assumed to be the intermediate stress and plane strain conditions in the axial direction are assumed. An explicit expression for the pressure–expansion relation is derived without any restriction imposed on the magnitude of the deformations. This is achieved by integrating the governing equation with the aid of a series expansion. Consequently, the limit cavity pressure when the radius of the cavity approaches infinity can be determined analytically with no additional assumption being made about the mode of deformation.

The importance of the new solution lies in the introduction of dilatancy into a complete large-strain analysis. Only approximate solutions to this problem have been published previously.

SOIL PROPERTIES

The properties of the soil are defined by the Young's modulus E and Poisson's ratio ν, and the cohesion, angle of friction and angle of dilation c, ϕ and ψ. The initial in situ stress (assumed isotropic) is p_0. The parameter m is used to indicate cylindrical analysis ($m = 1$) or spherical analysis ($m = 2$).

Several functions of these variables recur throughout the analysis and to abbreviate the mathematics it is convenient to define the following quantities, all of which are constant in any given analysis.

$$G = \frac{E}{2(1 + \nu)} \tag{1}$$

$$M = \frac{E}{1 - \nu^2(2 - m)} \tag{2}$$

$$Y = \frac{2c \cos \phi}{1 - \sin \phi} \tag{3}$$

$$\alpha = \frac{1 + \sin \phi}{1 - \sin \phi} \tag{4}$$

$$\beta = \frac{1 + \sin \psi}{1 - \sin \psi} \tag{5}$$

$$\gamma = \frac{\alpha(\beta + m)}{m(\alpha - 1)\beta} \tag{6}$$

$$\delta = \frac{Y + (\alpha - 1)p_0}{2(m + \alpha)G} \tag{7}$$

$$\eta = \exp\left\{\frac{(\beta + m)(1 - 2\nu) \times [Y + (\alpha - 1)p_0][1 + (2 - m)\nu]}{E(\alpha - 1)\beta}\right\} \tag{8}$$

$$\xi = \frac{[1 - \nu^2(2 - m)](1 + m)\delta}{(1 + \nu)(\alpha - 1)\beta} \times \left[\alpha\beta + m(1 - 2\nu) + 2\nu - \frac{m\nu(\alpha + \beta)}{1 - \nu(2 - m)}\right] \tag{9}$$

PROBLEM DEFINITION

An unbounded three-dimensional medium of dilatant soil contains a single cylindrical or spherical cavity. Initially the radius of the cavity is a_0 and a hydrostatic pressure p_0 acts throughout the soil, which is assumed to be homogeneous. The pressure inside the cavity is then increased to p sufficiently slowly for dynamic effects to be negligible. The major concern of this Paper is the distribution of stress and displacement in the soil as the pressure increases from p_0 to some limiting value.

The soil is modelled as an isotropic dilatant elastic–perfectly plastic material. It behaves elastically and obeys Hooke's law until the onset of yielding which is determined by the Mohr–Coulomb criterion. When the principal stress components satisfy the inequalities $\sigma_i \leqslant \sigma_j \leqslant \sigma_k$, the Mohr–Coulomb yield function takes the form

$$\alpha\sigma_k - \sigma_i = Y \tag{10}$$

in which α and Y are defined by equations (4) and (3) respectively. Tensile stresses and strains are taken as positive.

The initial position of a particle of soil is specified by spherical polar co-ordinates (r_0, θ, w) for a spherical cavity and by cylindrical polar co-ordinates (r_0, θ, z) for a cylindrical cavity. Plane strain conditions in the z direction are assumed for the cylindrical cavity. In addition, the vertical stress σ_z is assumed to be the intermediate principal stress and therefore there is no component of plastic strain in the vertical direction. This is because the plastic potential, which takes the form $\beta\sigma_k - \sigma_i = \text{constant}$, does not depend on the intermediate stress. These two assumptions are sufficient to determine the vertical stress as long as the other two stress components are known. This can be achieved simply by calculating the increase in σ_z in both elastic and plastic zones from the equation

$$\dot{\sigma}_z = \nu(\dot{\sigma}_r + \dot{\sigma}_\theta) \tag{11}$$

where ν denotes Poisson's ratio. The implication of these two assumptions will be discussed at length later in this Paper.

Before any additional pressure is applied within the cavity wall ($t = 0$), the cavity has a radius a_0 and an internal pressure p_0. At time t the cavity pressure has been increased to p and the cavity radius increased to a. A typical material point now has moved to radius r from r_0. In the current configuration the total stress must be in equilibrium. Because of symmetry this requirement can be expressed as

$$\sigma_\theta = \sigma_r + \frac{r}{m}\frac{\partial\sigma_r}{\partial r} \tag{12}$$

subject to the two boundary conditions:

$$\sigma_r(a) = -p \tag{13}$$

$$\lim_{r \to \infty} \sigma_r = -p_0 \tag{14}$$

noting that the convention of tension positive is used in this Paper.

The displacement, defined by

$$u = r - r_0 \tag{15}$$

is purely radial. As soils are characterized by the strong inequality $Y \ll E$ for both total stress undrained analysis and effective stress drained analysis, the use of small-strain theory for the initial phase of elastic deformation is justified provided also that $p_0 \ll E$, because the strain to the initiation of plasticity is then small. Following Gibson & Anderson (1961) and Houlsby & Withers (1988), a combination of a large-strain analysis in the plastic region and a small-strain solution in the elastic region is adopted in this Paper.

ELASTIC RESPONSE

As the applied pressure p increases from p_0, the deformation of the soil at first is purely elastic. Under conditions of radial symmetry the elastic stress–strain relationship may be expressed as

$$\dot{\varepsilon}_r = \frac{\partial\dot{u}}{\partial r} = \frac{1}{M}\left\{\dot{\sigma}_r - \frac{m\nu}{1 - \nu(2 - m)}\dot{\sigma}_\theta\right\} \tag{16}$$

$$\dot{\varepsilon}_\theta = \dot{\varepsilon}_\omega = \frac{\dot{u}}{r} = \frac{1}{M}\left\{-\frac{\nu}{1 - \nu(2 - m)}\dot{\sigma}_r + [1 - \nu(m - 1)]\dot{\sigma}_\theta\right\} \tag{17}$$

where the vertical strain for a cylindrical cavity is assumed to be zero. The solution of equations (16), (17) and (12) subject to the boundary conditions (13) and (14) is well known and can easily be shown to be

$$\sigma_r = -p_0 - (p - p_0)\left(\frac{a}{r}\right)^{m+1} \tag{18}$$

$$\sigma_\theta = -p_0 + \frac{p - p_0}{m}\left(\frac{a}{r}\right)^{m+1} \tag{19}$$

$$u = \frac{p - p_0}{2mG}\left(\frac{a}{r}\right)^{m+1} r \tag{20}$$

where G is the shear modulus. Since a compressive negative notation is used, the yield equation takes the form:

$$\alpha\sigma_\theta - \sigma_r = Y \tag{21}$$

As the pressure p increases further, initial yielding starts at the cavity wall when the condition

$$p = p_1 = \frac{m[Y + (\alpha - 1)p_0]}{m + \alpha} + p_0$$
$$= 2mG\delta + p_0 \tag{22}$$

is satisfied.

We shall now discuss the consistency of the stress and strain assumptions in the axial direction used for the expansion of a cylindrical cavity. The assumption of plane strain conditions and the intermediacy of σ_z results in two relationships between stresses in the plastic zone. They are defined by equation (11) and equation (21). Before the soil becomes plastic, the radial stress decreases while the hoop stress increases and the vertical stress remains unchanged. Once the soil deforms plastically all three stresses start to decrease. The relative magnitude of the decrease in each stress can easily be derived from equation (11) and equation (21) thus

$$\frac{\dot\sigma_z}{\dot\sigma_r} = \frac{2\nu}{1 + \sin\phi} \geqslant 0 \tag{23}$$

$$\frac{\dot\sigma_\theta}{\dot\sigma_r} = \frac{1 - \sin\phi}{1 + \sin\phi} \geqslant 0 \tag{24}$$

From equations (23) and (24) we can conclude that a sufficient condition for σ_z to remain as the intermediate stress is

$$\frac{\dot\sigma_z}{\dot\sigma_r} \geqslant \frac{\dot\sigma_\theta}{\dot\sigma_r} \tag{25}$$

which can be simplified further to

$$2\nu \geqslant 1 - \sin\phi \tag{26}$$

The condition defined by equation (26) breaks down only when both the Poisson's ratio and the friction angle of a soil are small. Even if this condition is violated, then the assumption that the axial stress remains intermediate may still be valid throughout the analysis since even though σ_z is approaching σ_θ it may not reach it before the end of the analysis. The most stringent test of this is in the calculation of limit pressures. For example, in an analysis where $G/p_0 = 100$, $\phi = 30^0$ and $\psi = 0^0$, it is found that the axial stress remains intermediate provided that $\nu > 0{\cdot}189$, whereas the strict criterion above would require $\nu > 0{\cdot}25$. The assumption about the axial stress will therefore be satisfied for most realistic values of soil parameters.

ELASTIC–PLASTIC STRESS ANALYSIS

After initial yielding at the cavity wall a plastic zone within the region $a \leqslant r \leqslant b$ forms around the inner wall of the cavity with the increase of the cavity pressure p. We now consider the plastic and elastic regions of the soil separately.

The plastic region $a \leqslant r \leqslant b$

The stress components which satisfy the equilibrium equation (12) and yield condition (21) can be found to be

$$\sigma_r = \frac{Y}{\alpha - 1} + Ar^{[-m(\alpha-1)]/\alpha} \tag{27}$$

$$\sigma_\theta = \frac{Y}{\alpha - 1} + \frac{A}{\alpha} r^{[-m(\alpha-1)]/\alpha} \tag{28}$$

where A is a constant of integration.

The elastic region $r \geqslant b$

The stress components in the elastic zone may be obtained from equations (12)–(14), (16) and (17) thus

$$\sigma_r = -p_0 - Br^{-(1+m)} \tag{29}$$

$$\sigma_\theta = -p_0 + (1/m)Br^{-(1+m)} \tag{30}$$

where B is a second constant. The continuity of stress components at the elastic–plastic interface can be used to determine the constants A and B in terms of the interface radius b

$$A = -\frac{(1 + m)\alpha[Y + (\alpha - 1)p_0]}{(\alpha - 1)(m + \alpha)} b^{[m(\alpha-1)]/\alpha}$$
$$= -\frac{(1 + m)\alpha}{\alpha - 1} 2\delta G b^{[m(\alpha-1)]/\alpha} \tag{31}$$

$$B = \frac{m[Y + (\alpha - 1)p_0]}{m + \alpha} b^{1+m} = 2m\delta G b^{1+m} \tag{32}$$

Combining equations (13) and (27) allows the elastic–plastic interface radius to be expressed in terms of the cavity pressure ratio R and the current cavity radius a

$$(b/a) = R^{\alpha/[m(\alpha-1)]} \tag{33}$$

where the cavity pressure ratio R is defined by

$$R = \frac{(m+\alpha)[Y + (\alpha - 1)p]}{\alpha(1+m)[Y + (\alpha - 1)p_0]} \tag{34}$$

The stresses are now established in terms of a single unknown b. In the next section the displacements are examined, allowing determination of b and therefore of the complete pressure–expansion relationship.

ELASTIC–PLASTIC DISPLACEMENT ANALYSIS

The results obtained above cannot be used to calculate the distribution of stress until the displacement field is known. On substituting from equations (29), (30) and (32) into equation (17) the displacement in the elastic zone $r \geqslant b$ can be shown to be

$$u = \delta\left(\frac{b}{r}\right)^{1+m} r \tag{35}$$

where δ is given by equation (7). The determination of the displacement field in the plastic zone requires the use of a plastic flow rule which indicates the relative magnitude of plastic strains in different directions. It is assumed that while yield is occurring, the total strain is decomposed into additive elastic and plastic components. Indices e and p are used to distinguish the elastic and plastic components of the total strains. Following Davis (1969), the soil is assumed to dilate plastically at a constant rate. This non-associated flow rule with the Mohr–Coulomb yield criterion is well established for modelling dilatant soil behaviour. Clearly the use of a fixed angle of dilation is a simplification and it would be preferable to consider the angles of friction and dilation as functions of density and pressure. This would, however, result in even more complex mathematics. The constant angle of dilation is at least a step forward from previous large-strain analyses in which zero dilation was assumed. For the loading phase of the cavity expansion the non-associated flow rule may be expressed as

$$(\dot{\varepsilon}_r^p / \dot{\varepsilon}_\theta^p) = -(m/\beta) \tag{36}$$

where β is defined in equation (5). If $\beta = \alpha$ then the flow rule for the soil is associated.

Substituting equations (16) and (17) into the plastic flow rule defined by equation (36) results in

$$\beta\dot{\varepsilon}_r + m\dot{\varepsilon}_\theta = \frac{1}{M}\left\{\left[\beta - \frac{mv}{1 - v(2-m)}\right]\dot{\sigma}_r + \left[m(1-2v) + 2v - \frac{m\beta v}{1 - v(2-m)}\right]\dot{\sigma}_\theta\right\} \tag{37}$$

where M is defined by equation (2). The distributions of stress and strain in the soil at the initiation of plastic yield are obtained from equations (16)–(20) by putting $p = p_1$. The integral of equation (37) subject to these conditions is found to be

$$\beta\varepsilon_r + m\varepsilon_\theta = \frac{1}{M}\left\{\left[\beta - \frac{mv}{1 - v(2-m)}\right]\sigma_r + \left[m(1-2v) + 2v - \frac{\beta m v}{1 - v(2-m)}\right]\sigma_\theta + \left[\beta + m(1-2v) + 2v - \frac{mv(1+\beta)}{1 - v(2-m)}\right]p_0\right\} \tag{38}$$

In order to account for effects of large strain in the plastic zone the logarithmic strain is adopted, namely

$$\varepsilon_r = \ln(dr/dr_0) \tag{39}$$

$$\varepsilon_\theta = \ln(r/r_0) \tag{40}$$

Substituting equations (39) and (40), and (27), (28) and (31) into equation (38) leads to

$$\ln\left[\left(\frac{r}{r_0}\right)^{m/\beta}\frac{dr}{dr_0}\right] = \ln\eta - \xi\left(\frac{b}{r}\right)^{[m(\alpha-1)]/\alpha} \tag{41}$$

where η and ξ are defined by equations (8) and (9) respectively.

By means of the transformation

$$\rho = (b/r)^{[m(\alpha-1)]/\alpha} \tag{42}$$

$$\zeta = (r_0/b)^{(\beta+m)/\beta} \tag{43}$$

and use of equation (35), equation (41) can be integrated over the interval $[b, r]$, leading to

$$\frac{\eta}{\gamma}\{(1-\delta)^{(\beta+m)/\beta} - (r_0/b)^{(\beta+m)/\beta}\} = \int_1^{(b/r)[m(\alpha-1)]/\alpha} \exp(\xi\rho)\rho^{-\gamma-1}\,d\rho \tag{44}$$

By putting $r_0 = a_0$, $r = a$ and making use of equation (33), we have

$$\frac{\eta}{\gamma}\{(1-\delta)^{(\beta+m)/\beta} - R^{-\gamma}(a_0/a)^{(\beta+m)/\beta}\} = \int_1^R \exp(\xi\rho)\rho^{-\gamma-1}\,d\rho \tag{45}$$

For spherical cavity expansion in the associated Mohr–Coulomb material (i.e. $m = 2$ and $\beta = \alpha$) equation (45) reduces to the solution given by Chadwick (1959).

With the aid of the series expansion

$$\exp(\xi\rho) = \sum_{n=0}^{\infty} \frac{(\xi\rho)^n}{n!} \tag{46}$$

the following explicit expression for the pressure–expansion relationship is obtained

$$\frac{a}{a_0} = \left\{\frac{R^{-\gamma}}{(1-\delta)^{(\beta+m)/\beta} - (\gamma/\eta)\Lambda_1(R, \xi)}\right\}^{\beta/(\beta+m)} \tag{47}$$

where

$$\Lambda_1(x, y) = \sum_{n=0}^{\infty} A_n^1 \tag{48}$$

in which

$$A_n^1 = \begin{cases} \dfrac{y^n}{n!} \ln x & \text{if} \quad n = \gamma \\ \dfrac{y^n}{n!(n-\gamma)} [x^{n-\gamma} - 1] & \text{otherwise} \end{cases}$$

and the first condition will only rarely be encountered since γ is unlikely to take an integer value.

Having noted that ξ is a small value with the same order as δ, we can easily prove that the series defined by equation (48) converges very rapidly for all values of α and β of the soil. In general, the first few terms in the series may be used to give satisfactory results.

All the necessary information is now available to construct the complete pressure–expansion curve, but it is not expressed in terms of a single equation. It is worth summarizing the procedure to be used to construct the curve:

(*a*) choose input parameters E, v, c, ϕ, ψ, p_0 and m
(*b*) calculate the derived parameters G, M, α, β, Y, γ, δ, η and ξ from equations (1) to (9)
(*c*) for pressure p less than the pressure p_1 required to initiate plasticity, equation (22), calculate the cavity radius from the small-strain elastic expression $(a - a_0)/a_0 = (p - p_0)/2mG$
(*d*) for a given value of p (greater than p_1 and less than the limit pressure p_∞ discussed below) calculate R from equation (34)
(*e*) evaluate sufficient terms in the infinite series in equation (48) to obtain an accurate value of Λ_1—only a few terms will usually be sufficient
(*f*) evaluate a/a_0 from equation (47) and if necessary the pressuremeter displacement $u = a - a_0$ or the hoop strain at the cavity surface $\varepsilon = \ln(a/a_0)$.

The procedure from (*d*) to (*f*) can be repeated to construct the complete cavity pressure–expansion relationship.

It is worth noting that at the transition from elastic to plastic behaviour one can calculate from the plastic expressions that $R = 1$ and $\Lambda_1 = 0$ so that $p = p_0 + 2mG\delta$ and $a/a_0 = 1/(1-\delta)$. Only if δ is small (i.e. if small-strain theory is appropriate to the elastic region) does this reduce to the same solution as for elasticity. The following form is a convenient alternative expression for δ

$$\delta = \frac{c\cos\phi + p_0 \sin\phi}{G[(1+m) + (1-m)\sin\phi]} \tag{49}$$

For typical soil parameters δ is unlikely to take a value larger than about 1/200.

SPECIAL CASES

Limit pressure

When a cavity is expanded in a plastically deforming material the cavity pressure does not increase indefinitely, but a limit pressure is approached. By putting $(a/a_0) \to \infty$ in equation (47), the limit cavity pressure p_∞ may be obtained by finding R_∞ from

$$\Lambda_1(R_\infty, \xi) = (\eta/\gamma)(1-\delta)^{(\beta+m)/\beta} \tag{50}$$

where

$$R_\infty = \frac{(m+\alpha)[Y + (\alpha - 1)p_\infty]}{\alpha(1+m)[Y + (\alpha-1)p_0]} \tag{51}$$

It was found that the limit pressure depends strongly on both the angle of friction and the angle of dilation, as well as the stiffness properties of the soil. A discussion of the variation of limit pressure and some implications in geotechnical engineering is given in a later section.

Frictionless case

The importance of the solution above is for its application to soils with friction and dilation. The above solution does not reduce to the solution for a frictionless soil when $\phi = 0$. This is because in this case $\alpha = 1$ and the terms in $(\alpha - 1)$ which frequently appear in the denominator make the expressions indeterminate. For $\phi = 0$, $\psi = 0$ and $v = 0{\cdot}5$ the plastic solution is (Gibson & Anderson, 1961)

$$p = p_0 + \frac{2+m}{3} c\{1 + \ln(G/c) + \ln[1 - (a_0/a)^{m+1}]\} \tag{52}$$

Since the application of the $\phi = 0$ solution is to undrained analysis, it is unlikely that a solution with different values of ψ and ν will be of practical interest. It can be confirmed that at very small ϕ values the solution presented in this Paper approaches numerically the values given by equation (52).

Small strain case

Large-strain theory is somewhat complex and, where possible, small-strain theory is used to model cavity expansion. In small-strain theory the fact that the displacements modify the position of material points is ignored, so the theory is only valid for small expansions. In particular, no prediction of limit pressure is possible using small-strain theory. It can be shown that if the small-strain assumption is made it is possible to obtain the following closed form expression for displacement in the plastic zone

$$u = \left[\delta + \frac{\alpha\beta\xi}{m(\alpha+\beta)+\alpha\beta(1-m)} - \frac{\beta \ln \eta}{\beta + m}\right]\left(\frac{b}{r}\right)^{m/\beta} b + \frac{\beta \ln \eta}{\beta+m} r - \frac{\alpha\beta\xi}{m(\alpha+\beta)+\alpha\beta(1-m)}\left(\frac{b}{r}\right)^{[m(\alpha-1)]/\alpha} r \quad (53)$$

Noting that the special case where $r = a_0$ gives the displacement at the pressuremeter surface, this equation can be used instead of equation (47), and is simpler because it is not necessary to evaluate the infinite series.

Equation (53) is only applicable to the situation where the maximum value of the cavity pressure is sufficiently small for the squares and higher powers of strains included in the large-strain definition (equations (39)–(40)) to be negligible. This small-strain solution is the same as that derived by Carter *et al.* (1986). When $\beta = \alpha$ and $m = 2$ the solution reduces to the case for spherical expansion given by Chadwick (1959).

Neglecting elastic strain in plastic zone

A common assumption which considerably simplifies the analysis of plastic cavity expansion (see for example Hughes *et al.*, 1977) is to ignore the contribution of elastic strain within the plastically deforming region. While this may at first seem to be a reasonable assumption, since the elastic strains are considerably smaller than the plastic strains, it appears that it has a significant effect on the predicted results.

Neglecting the elastic deformation in the plastic zone results in the relatively simple expression for R from which the large-strain pressure–expansion relationship can be derived

$$R = \left[\frac{1-(a_0/a)^{(\beta+m)/\beta}}{1-(1-\delta)^{(\beta+m)/\beta}}\right]^{1/\gamma} \quad (54)$$

Note that this again avoids the need to evaluate the infinite series. A comparison between the approximate solution obtained from equation (54) and the exact solution defined by equation (47) clearly indicates that the effects of elastic strain in the plastic zone are more important for soils with a high angle of friction, high angle of dilation and low elastic stiffness. This is exactly the trend that would be expected. By putting $a_0/a = 0$ and $\beta = 1$ and assuming δ is small, equation (54) reduces to the limit solution derived by Vesic (1972).

RESULTS

A selection of results is now presented in order to indicate the effects of the various parameters on the behaviour of cavity expansion. The pressure–expansion relationship, derived from the procedure described above is plotted in Fig. 1 for a material with a Poisson's ratio ν of 0·3, a friction angle ϕ of 30° and a stiffness index $E/\{p_0 + [Y/(\alpha-1)]\}$ of 260. Three curves are shown for ψ values of 0°, 15° and 30°. The expansion pressure is expressed non-dimensionally as $(p + c \cot \phi)/(p_0 + c \cot \phi)$. The increasing stiffness of the response with increasing dilatancy is clearly shown. For the range of expansion ratios a/a_0 shown up to 1·2, a small-strain theory would give similar results, but at larger expansion ratios a large-strain theory is necessary. The same analyses are shown continuing to an expansion ratio of 10 in Fig. 2, in which the limit pressure which is approached asymptotically is clearly shown. The limit pressure is seen to depend strongly on the angle of dilation, as higher angles of dilation result in a more extensive plastically

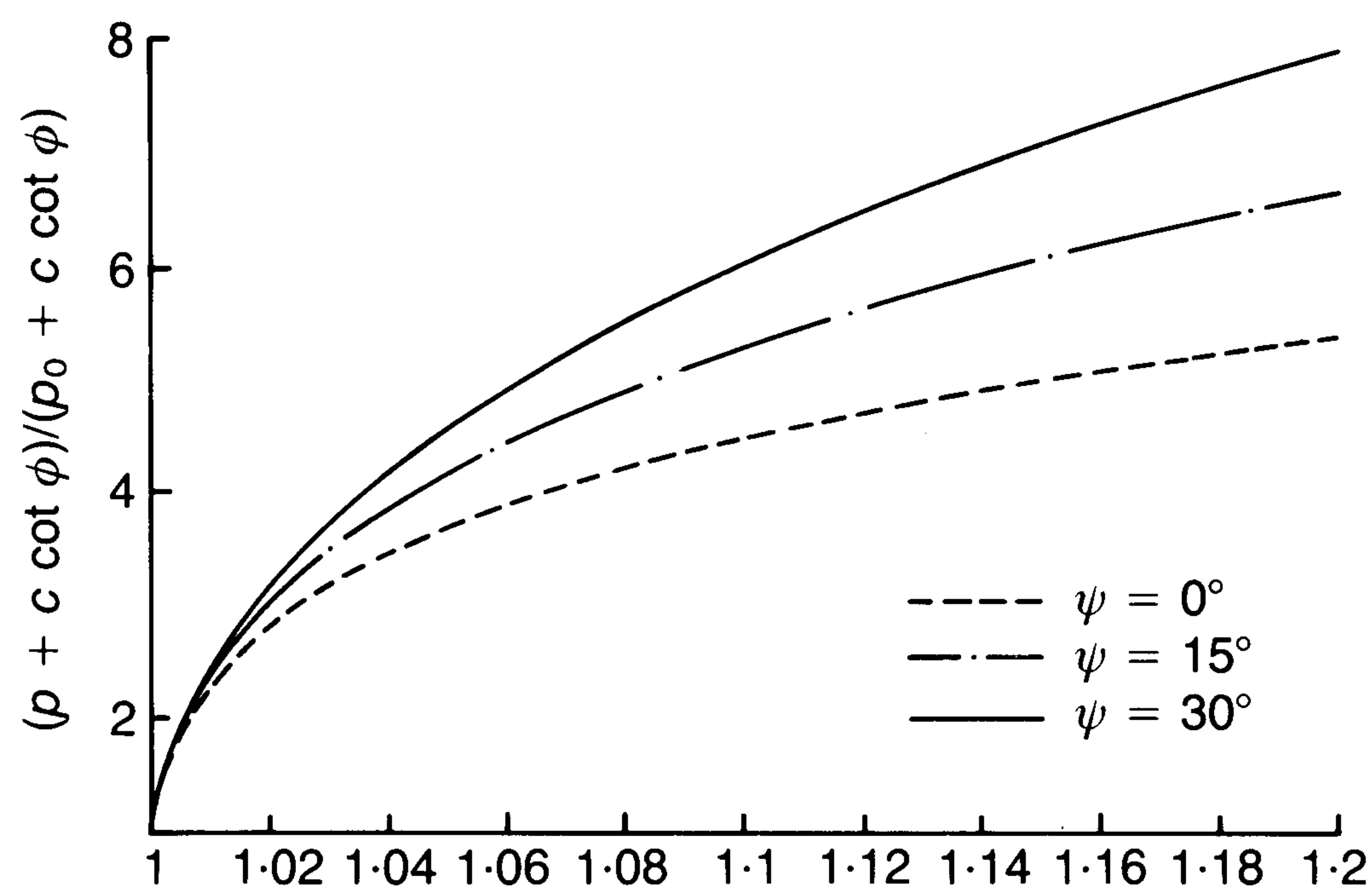

Fig. 1. Typical pressure–expansion curves for cylindrical cavities—initial section

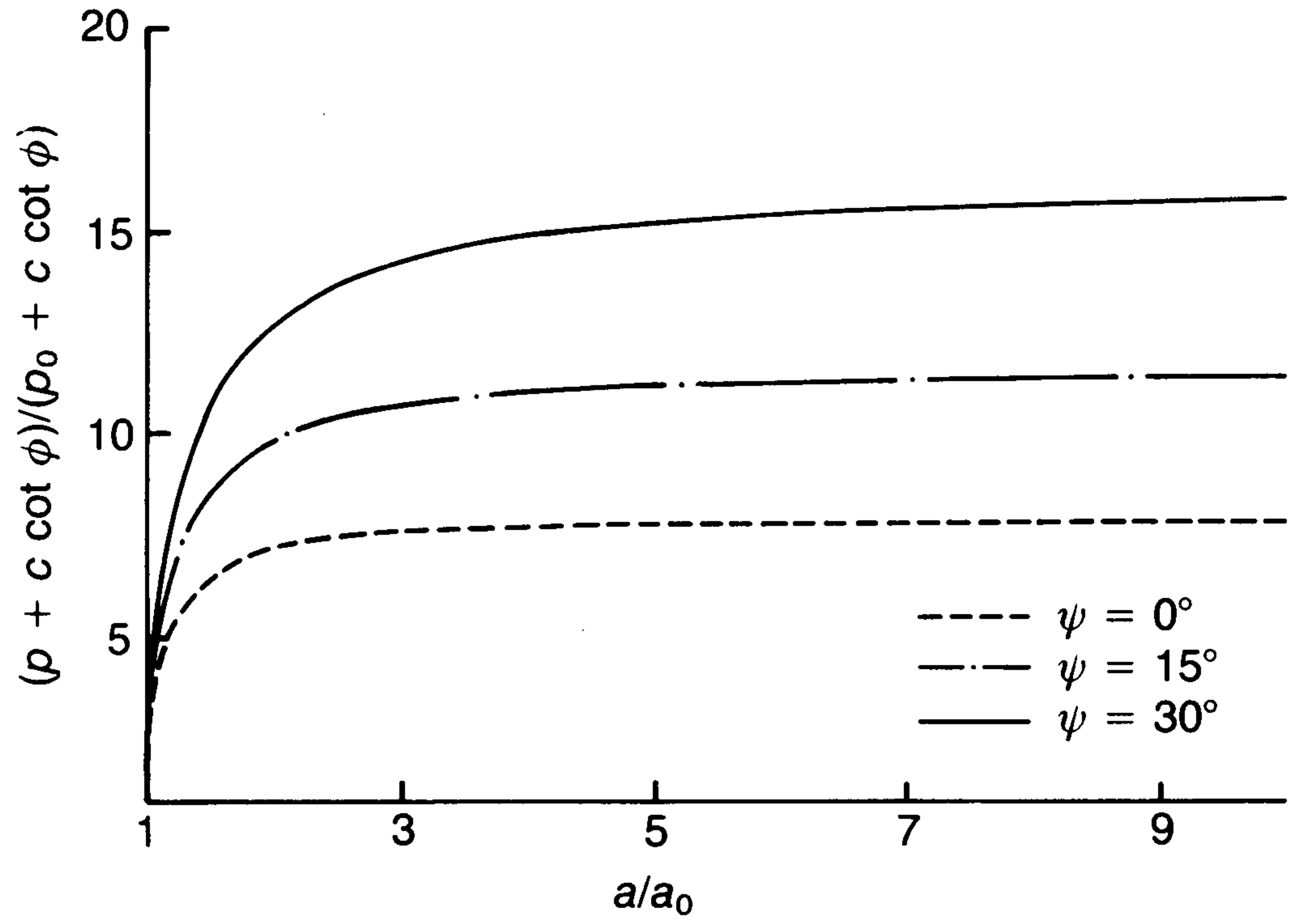

Fig. 2. Typical pressure–expansion curves for cylindrical cavities

deforming zone. Figs 3 and 4 show the equivalent results for spherical cavity expansion. The trend of the results is exactly as for cylindrical expansion, but the response is much stiffer and the limit pressures correspondingly higher.

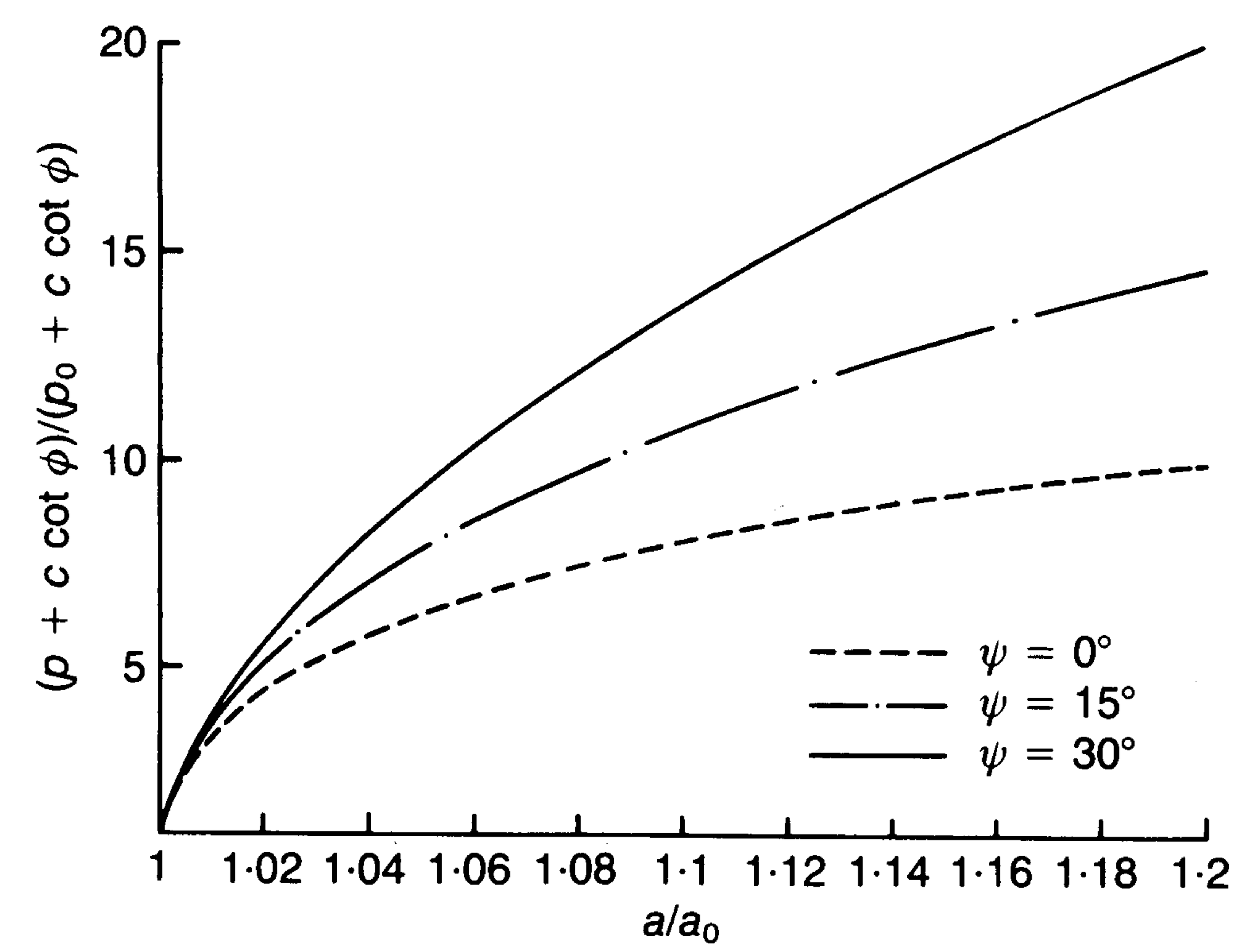

Fig. 3. Typical pressure–expansion curves for spherical cavities—initial section

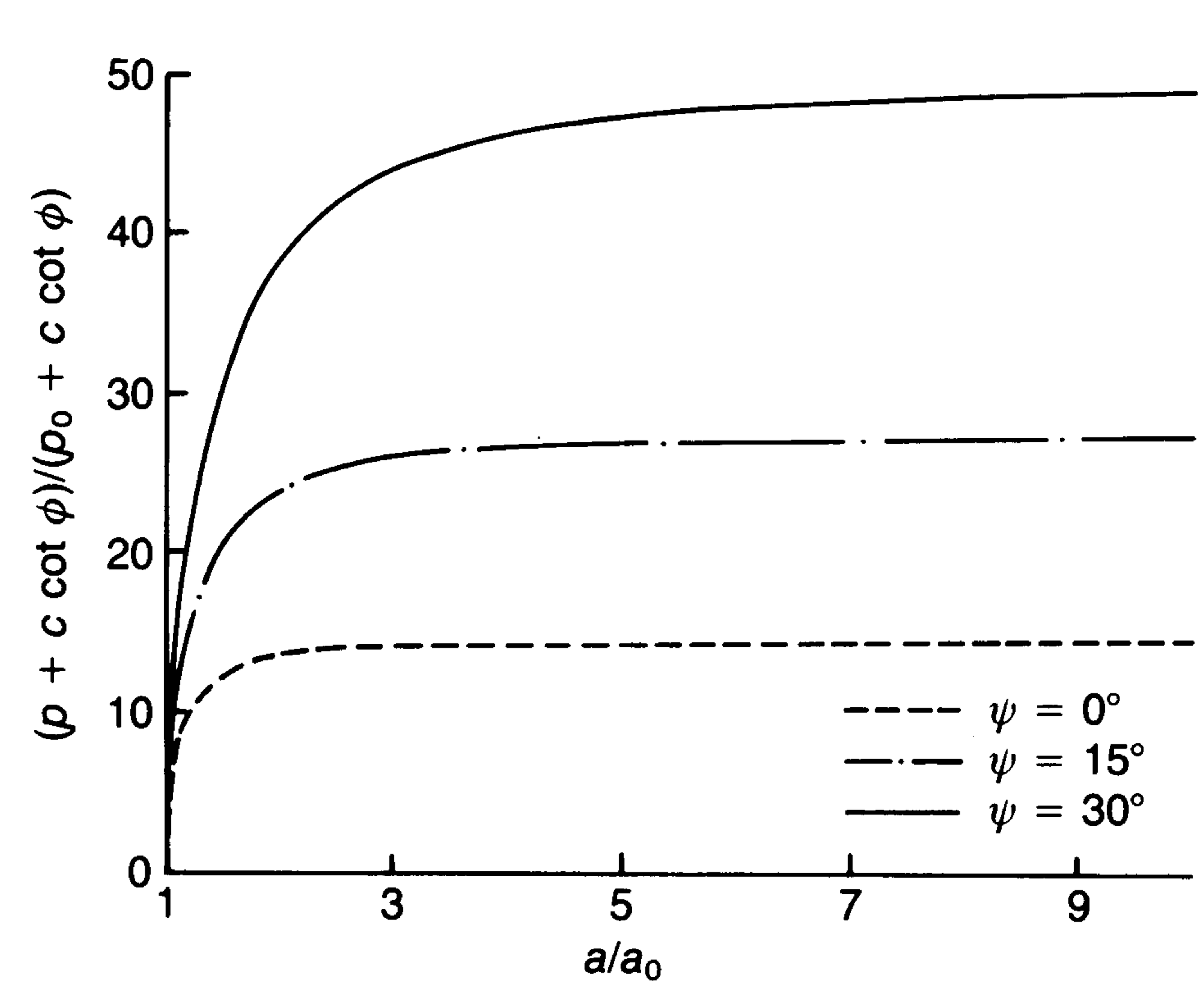

Fig. 4. Typical pressure–expansion curves for spherical cavities

The stresses calculated around an expanding cylindrical cavity, as defined by equations (27)–(32) at a cavity expansion ratio of 10 for a material with the properties defined above, $\psi = 0°$ and $Y = 0{\cdot}5p_0$ are presented in Fig. 5. The variable on the horizontal axis is a/r, so that the left side of the figure shows the stresses remote from the cavity and the right side shows the stresses close to the cavity. It can be seen that close to the cavity the radial stress is largest, the hoop stress smallest and the axial stress intermediate. Similar results are shown for a spherical cavity (with a ψ of 30°) in Fig. 6. In this case the rate of increase of the radial stress as the cavity is approached is even more striking.

Limit pressure solutions

One of the most important results from this Paper is the solution for limit pressures in dilatant soils. The limit pressure in spherical cavity expansion is often applied to estimate the end bearing capacity of piles or the tip resistance in

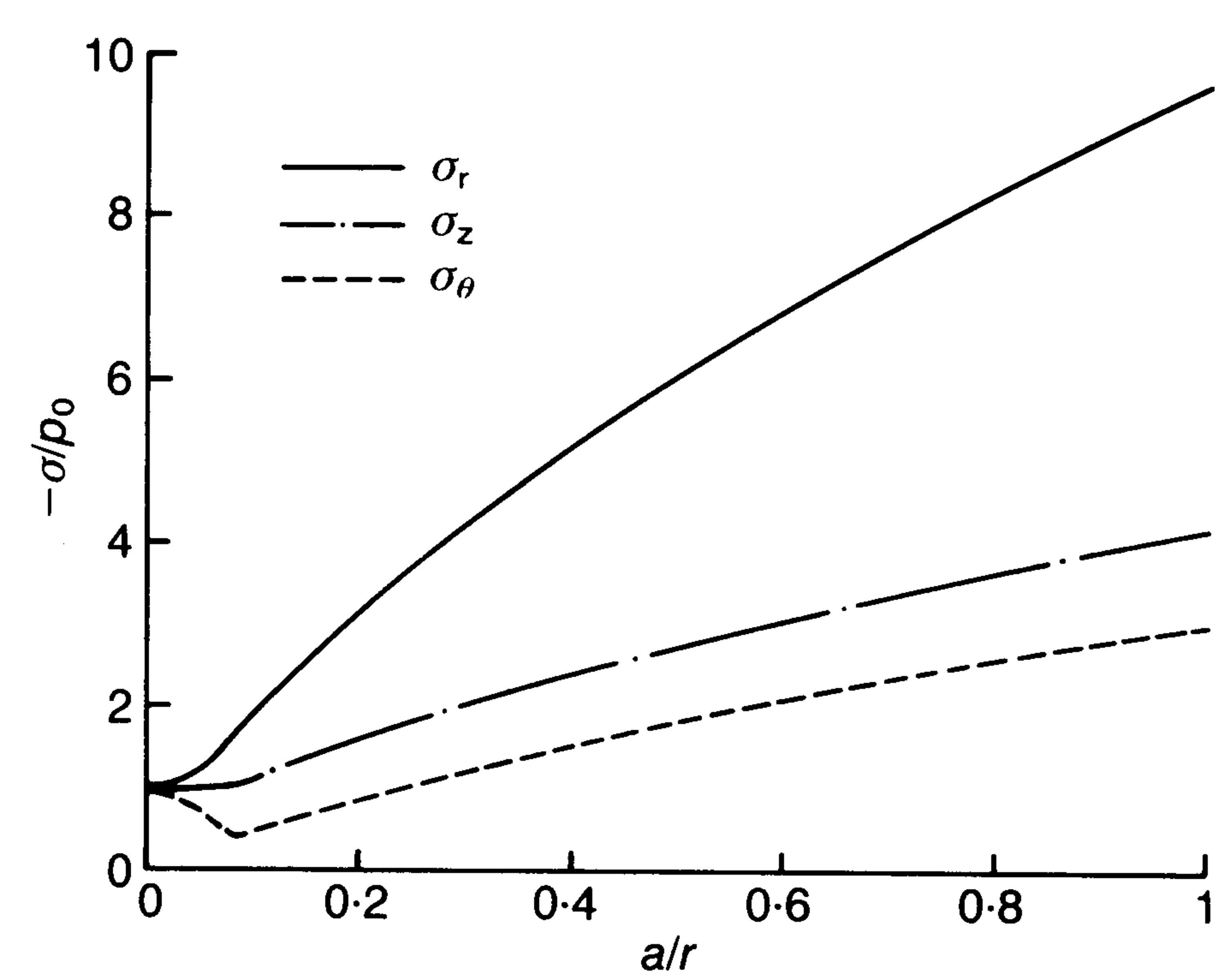

Fig. 5. Stress distribution around cylindrical cavity, $\psi = 0°$

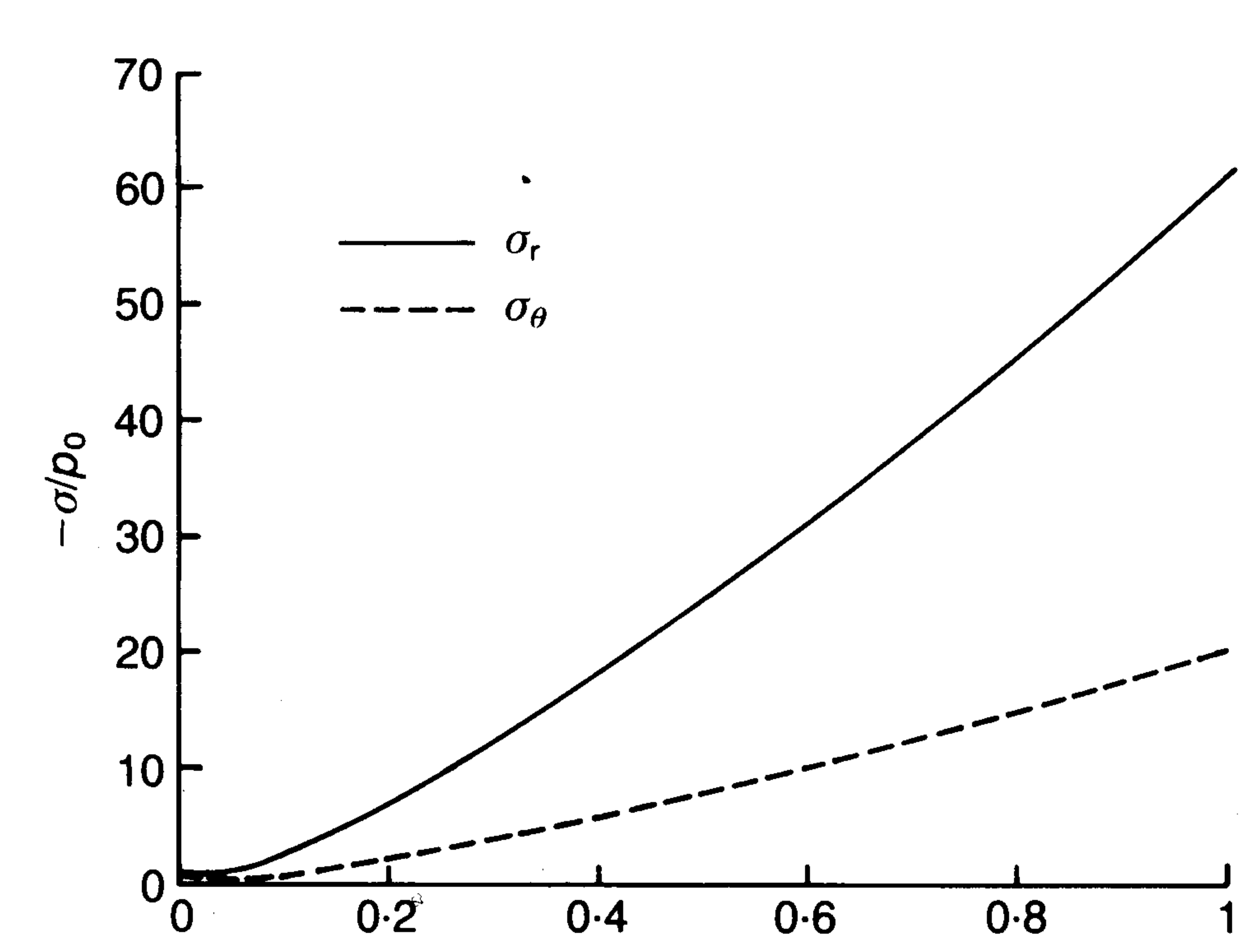

Fig. 6. Stress distribution around a spherical cavity, $\psi = 30°$

the cone penetrometer test. While this gives reasonable values for undrained problems (i.e. the frictionless case) it has been found that spherical limit pressures calculated using previously published solutions severely underestimate end bearing resistance in frictional materials.

In Fig. 7 the variation of limit pressure for both cylindrical and spherical expansion with friction angle is shown. The following values were used: $c = 0$, $\nu = 0{\cdot}2$ and $G/p_0 = 500$. For each case four curves are presented. Curves (a), (b) and (c) are for $\psi = 0°$, $10°$ and $20°$ respectively, while curve (d) shows a realistic variation for a single soil with $\phi_{cv} = 33°$ and $\phi = \phi_{cv} + 0{\cdot}8\psi$. It can be seen that the inclusion of dilation in the analysis has a very important effect, increasing the limit pressures considerably. For spherical cavity expansion the limit pressure for the realistic soil varies from about $31p_0$ in a very loose state ($\phi = 33°$) to about $353p_0$ in a very dense state ($\phi = 49°$). In the latter case, if dilation were to be ignored, then the limit pressure would be only $58p_0$.

The other primary variable which controls the limit pressure is the ratio of stiffness to strength of the soil, closely related to the inverse of the factor δ. In Fig. 8 the variation of limit pressure with G/p_0 is presented for the case $\phi = 40°$, and $\nu = 0{\cdot}2$. Values of ψ of $0°$, $10°$ and $20°$ are considered.

In analyses which neglect the elastic strains in the plastically deforming region then the only elastic property which influences the solution is the shear modulus G, but when this simplification is not made then the Poisson's ratio does influence the limit pressure. As shown in Fig. 9, the limit pressure does depend on the Poisson's ratio, particularly for the case of spherical expansion.

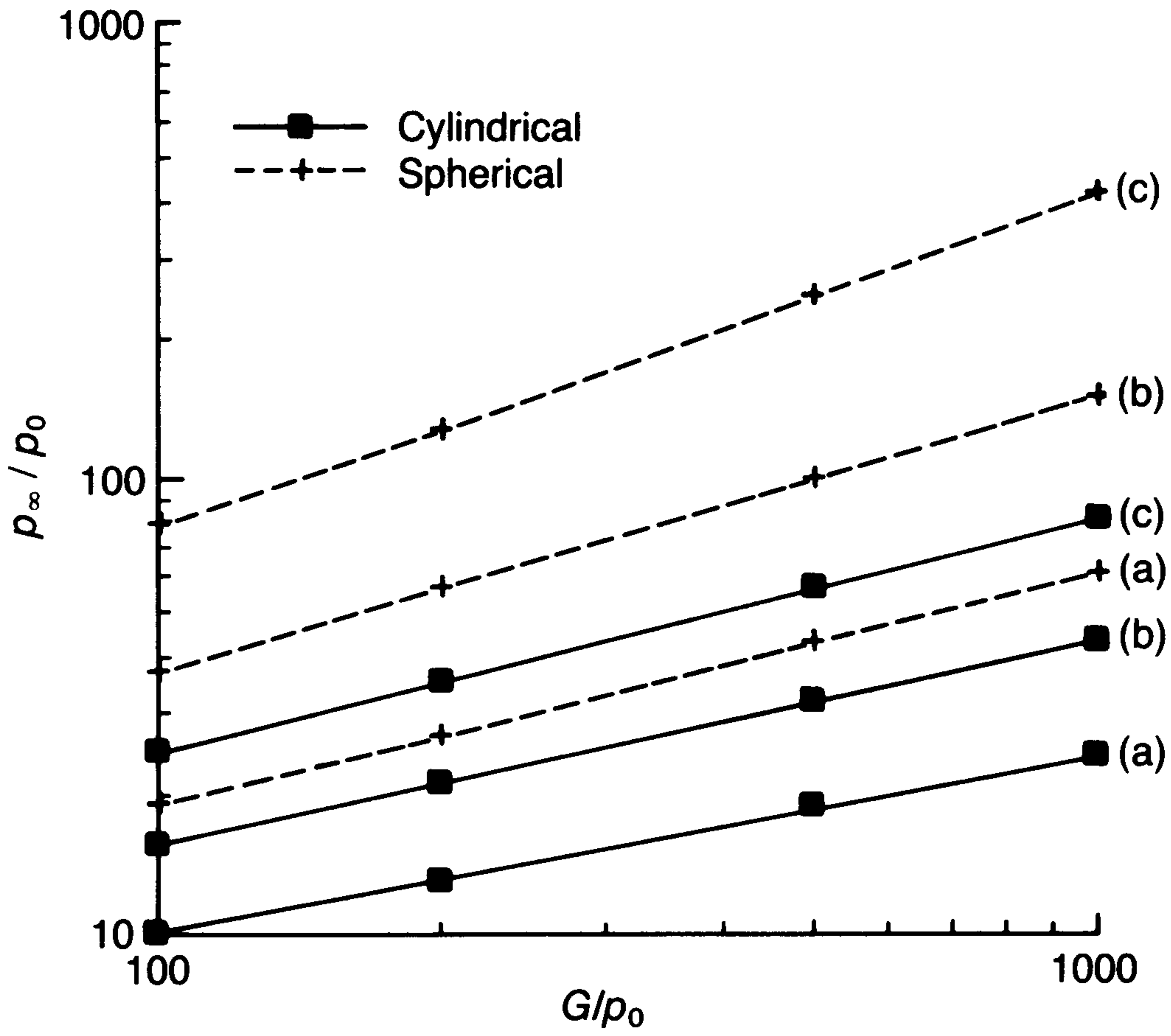

Fig. 8. Variation of limit pressure with stiffness, $\nu = 0{\cdot}2$, $\phi = 40°$: (a) $\psi = 0°$, (b) $\psi = 10°$, (c) $\psi = 20°$

Application to piling engineering

The fact that the inclusion of dilation significantly increases the limit pressure means that the spherical limit pressure can now realistically be applied to the estimation of pile end bearing capacity. Calculations of spherical limit pressure have been made for a typical quartz sand using the following estimates of soil properties.

The angles of friction and dilation are estimated from the correlations published by Bolton (1986): $\phi_{cv} = 33°$, $\phi = \phi_{cv} + 3[I_D(10 - \ln p') - 1]$ where I_D is the relative density and p' is the mean effective stress in kPa at failure. The dilation angle is given by $\phi = \phi_{cv} + 0{\cdot}8\psi$. The stiffness properties are $G/p_0 = 1000$ and $\nu = 0{\cdot}2$. Fig. 10 shows the predicted variation of spherical limit

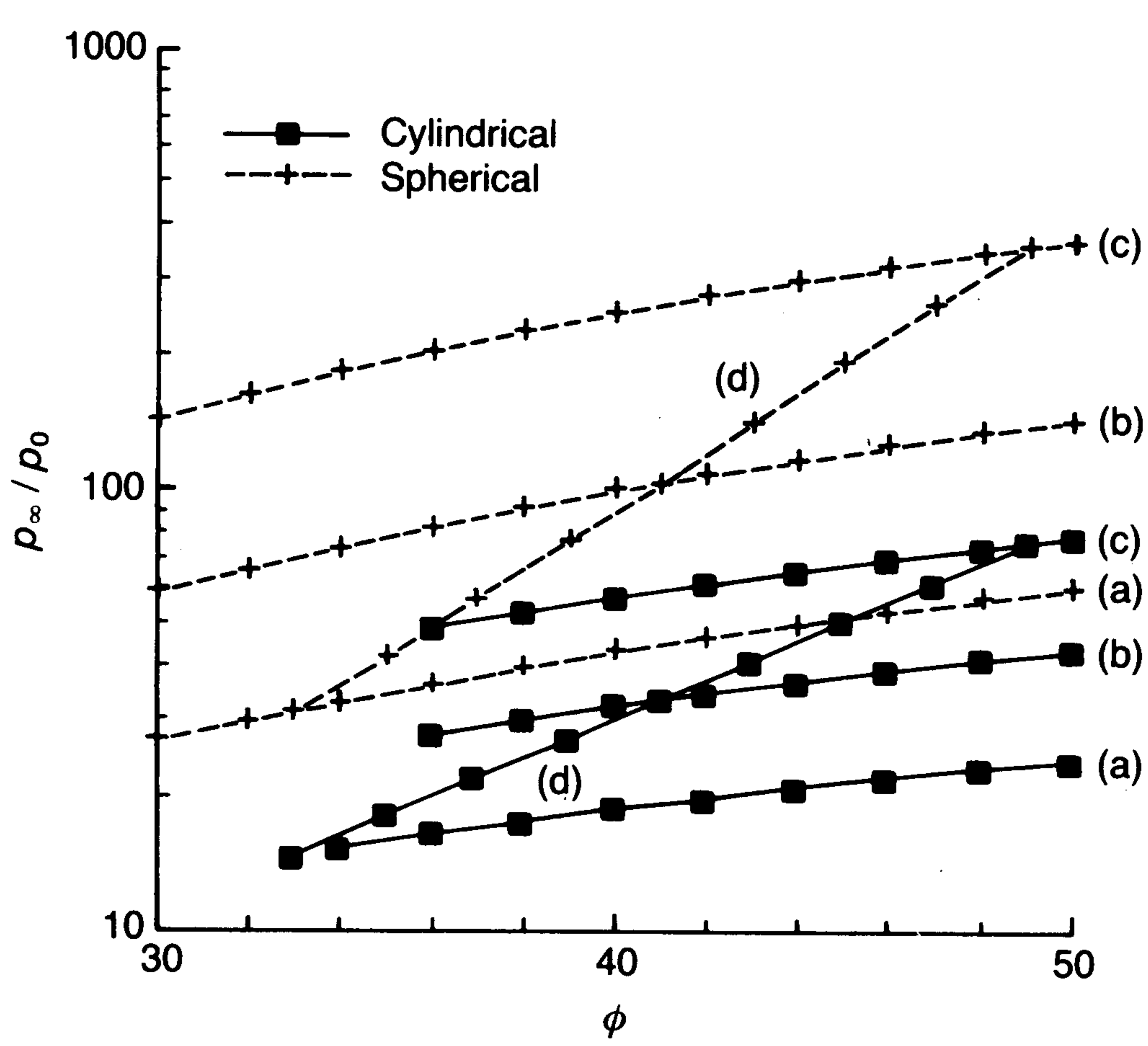

Fig. 7. Variation of limit pressure with angle of friction, $G/p_0 = 200$, $\nu = 0{\cdot}2$: (a) $\psi = 0°$, (b) $\psi = 10°$, (c) $\psi = 20°$, (d) $\phi = 33° + 0{\cdot}8\psi$

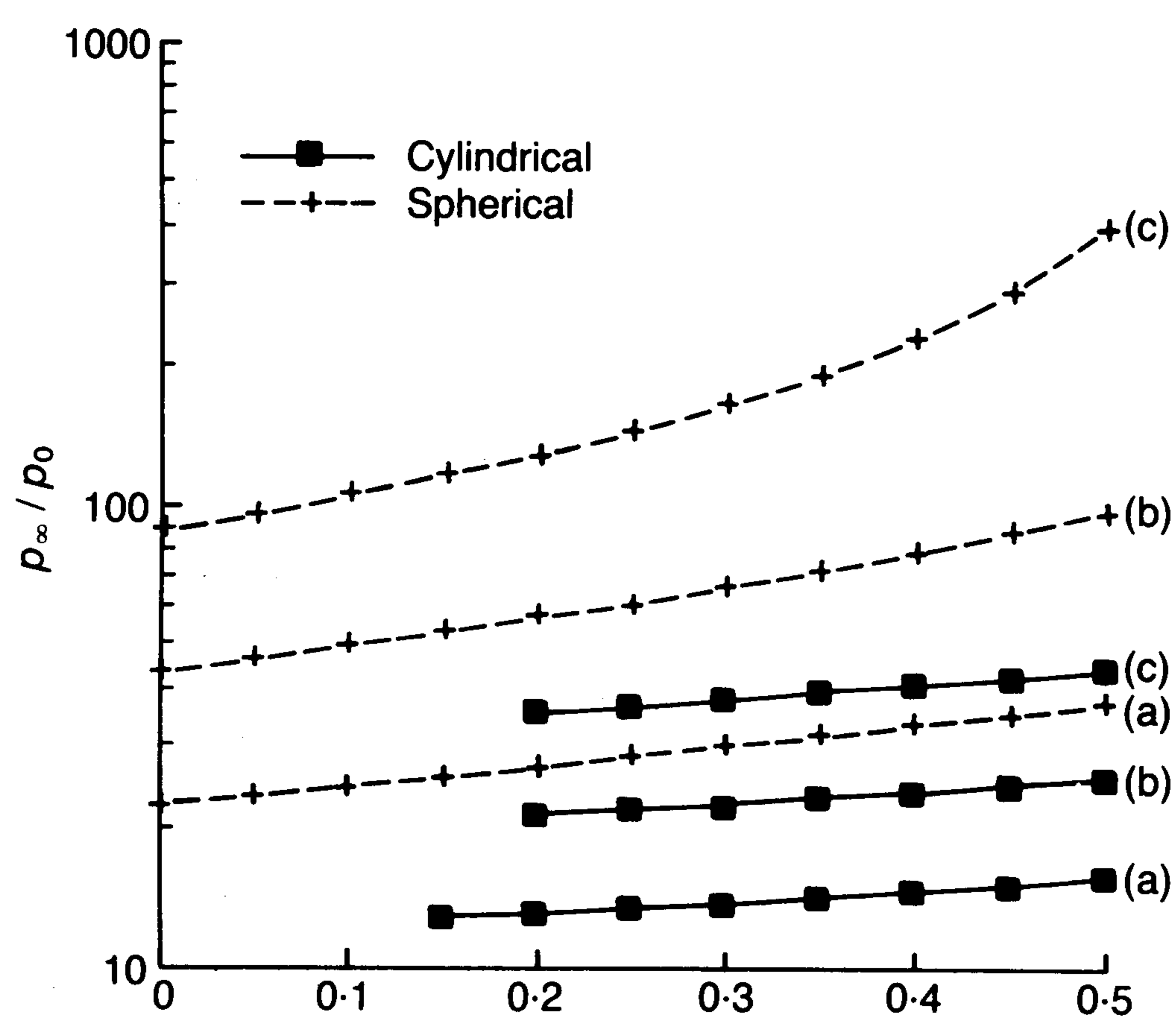

Fig. 9. Variation of limit pressure with Poisson's ratio, $G/p_0 = 200$ $\phi = 40°$: (a) $\psi = 0°$, (b) $\psi = 10°$, (c) $\psi = 20°$

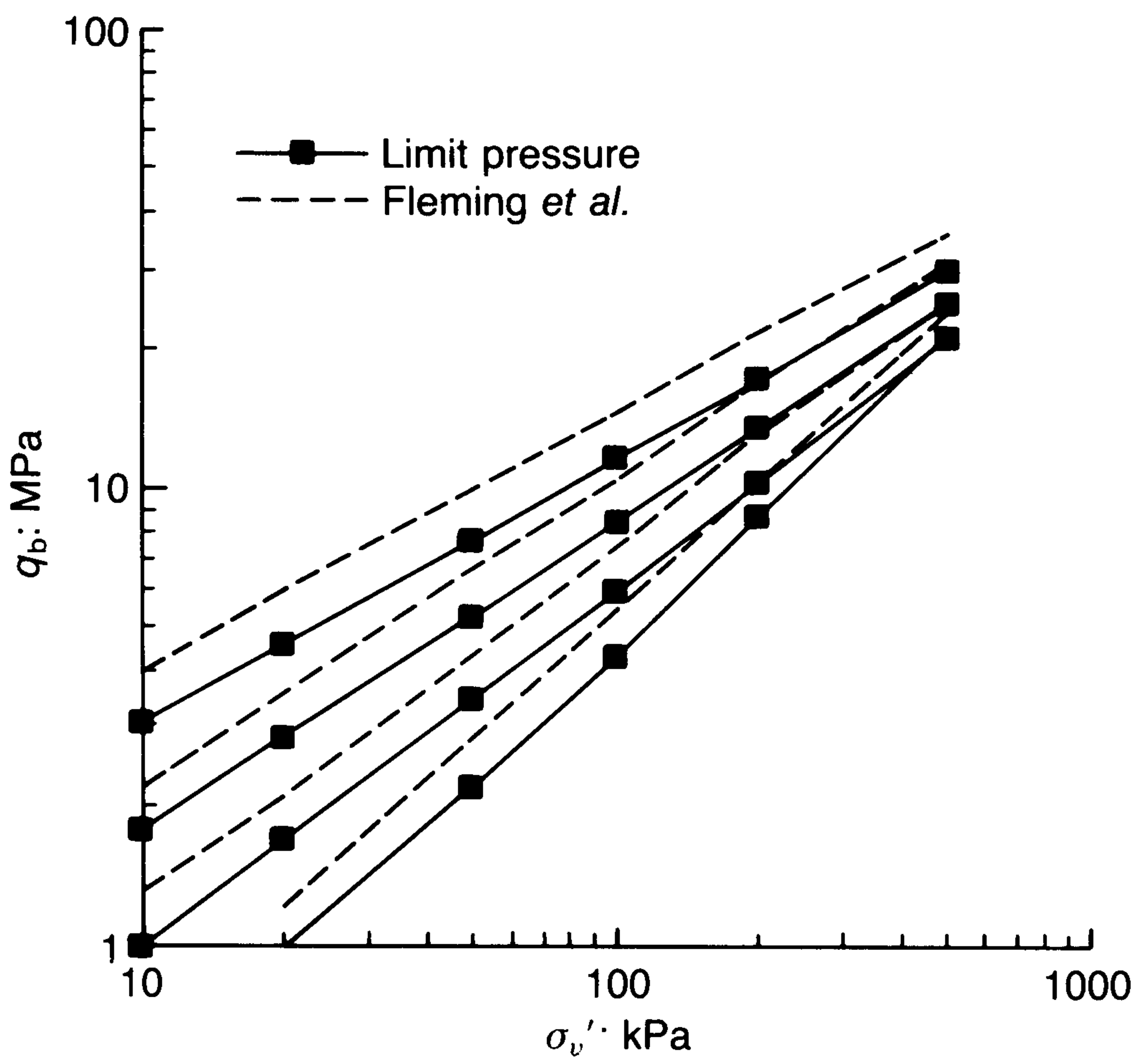

Fig. 10. End bearing capacity of piles calculated by limit pressure method, compared to chart given by Fleming *et al.* (1985), $\phi_{cv} = 33°$

pressure with relative density and vertical effective stress (taken as p_0 in this analysis since initial stresses are assumed isotropic). The p' value for Bolton's correlation is estimated iteratively as $p' = \sqrt{(p_0 p_\infty)}$. The spherical limit pressure may be compared to the results presented by Fleming *et al.* (1985) in their design chart for the end bearing capacity of piles. The latter figures were derived using estimates of ϕ and Berezantzev's approximate bearing capacity factors for buried circular footings. The comparison shows that the spherical limit pressure is comparable to accepted end bearing capacity values in sands. It is consistently lower than the values presented by Fleming *et al.* (1985) by a factor of about 0·8. This difference depends to a large extent on the specific choice of the G/p_0 value.

Future developments

The analysis described in this Paper also serves as the starting point for an analysis of the unloading of a cylindrical or spherical cavity after an initial loading phase. This is treated in a companion paper (Yu & Houlsby, 1991). The analysis of unloading is receiving increased attention as it is appreciated that additional information can be obtained from pressuremeter tests by examining the unloading as well as the loading phase of the test.

An obvious limitation of the analysis presented here is that the friction and dilation angles are assumed constant. As a dense soil dilates it approaches the critical state, the angle of dilation gradually approaches zero and the angle of friction approaches its critical state value. The angles of friction and dilation can be estimated with some accuracy if the stress level and the current density are known. It would be more realistic to model cavity expansion in dilatant soils using variable angles of dilation and friction, but the complexity of the mathematics is likely to become so great as to render closed form solutions impractical.

The most efficient way to progress will be to use numerical analysis for such cases, since the implementation of variable properties in, for instance, a finite element program is straightforward. A new approach for the accurate analysis of this type of problem has recently been developed (Yu & Houlsby, 1990). In this case the solutions obtained in this Paper play an important role in the calibration of the numerical analysis to verify that it is giving reliable solutions.

CONCLUSION

A unified analytical solution is presented for the stress and displacement fields for the expansion of both cylindrical and spherical cavities in dilatant soils. The approach using the direct integration of strain rate and the logarithmic strain definition has been used so that large-strain effects can be taken into account. The dilatancy of the soil is accounted for by adopting the Mohr–Coulomb yield criterion with a non-associated plastic flow rule. An explicit expression for the pressure–expansion relationship has been obtained for a displacement with arbitrary magnitude. The analytical limit pressure can then be determined as a special case when the cavity radius approaches infinity. Finally, some selected results are presented to highlight the capability of the proposed solutions.

ACKNOWLEDGEMENTS

The Authors are grateful to Professor C. P. Wroth for useful discussions and valuable comments. The comments made by Dr H. J. Burd are also very much appreciated.

NOTATION

a	radius of the cavity during loading
a_0	radius of the cavity at initial unloaded state
A, B	constants of integration
A_n^1	general term of infinite series
b	outer radius of the plastic zone during loading
c	cohesion of the soil
E	Young's modulus
G	shear modulus
m	factor identifying cavity type

M function of material properties
n integer from zero to infinity
p cavity pressure
p_0 initial cavity pressure and in-situ hydrostatic stress
p_∞ limit cavity pressure
p_1 cavity pressure causing first yielding
q_b pile end bearing capacity
r radius of a material point during loading
r_0 radius of material point at initial state
R cavity pressure ratio
R_∞ limit cavity pressure ratio
u radial displacement during loading measured from initial state
x, y auxiliary variables
Y function of cohesion and friction angle
z axial direction for cylindrical cavity
α function of friction angle
β function of dilation angle
γ function of material properties
δ function of material properties
$\varepsilon_r, \varepsilon_z\ \varepsilon_\theta$ strains measured from initial state
η function of material properties
Λ_1 infinite power series
ν Poisson's ratio
ξ function of material properties
ρ, ζ auxiliary variables
$\sigma_r, \sigma_z, \sigma_\theta$ stresses
ϕ friction angle
ψ dilation angle

REFERENCES

Bigoni, D. & Laudiero, F. (1989). The quasi-static finite cavity expansion in a non-standard elasto-plastic medium. *Int. J. Mech. Sci.* **31,** 825–838.

Bishop, R. F., Hill, R. & Mott, N. F. (1945). Theory of indentation and hardness tests. *Proc. Phys. Soc.* **57,** 147–159.

Bolton, M. D. (1986). The strength and dilatancy of sands. *Géotechnique* **36,** No. 1, 65–78.

Carter, J. P., Booker, J. R. & Yeung, S. K. (1986). Cavity expansion in cohesive frictional soils. *Géotechnique* **36,** No. 3, 349–353.

Carter, J. P. & Yeung, S. K. (1985). Analysis of cylindrical cavity expansion in a strain weakening material. *Computers and Geotechnics* **1,** 161–180.

Chadwick, P. (1959). The quasi-static expansion of a spherical cavity in metals and ideal soils. *Q. J. Mech. Appl. Math.* **12,** 52–71.

Davis, E. H. (1969). Theories of plasticity and the failure of soil masses. *Soil mechanics* (ed. I. K. Lee). London: Butterworths.

Fleming, W. G. K., Weltman, A. J., Randolph, M. F. & Elson, W. K. (1985). *Piling engineering.* Guildford: Surrey University Press.

Gibson, R. E. & Anderson, W. F. (1961). In-situ measurement of soil properties with the pressuremeter. *Civ. Engng Pub. Wks Rev.* **56,** 615–618.

Hill, R. (1950). *The mathematical theory of plasticity.* Oxford University Press.

Houlsby, G. T. & Withers, N. J. (1988). Analysis of the cone pressuremeter test in clay. *Géotechnique* **38,** 573–587.

Houlsby, G. T., Clarke, B. G. & Wroth, C. P. (1986). Analysis of the unloading of a pressuremeter in sand. *Proc. 2nd Int. Symp. on the Pressuremeter and its Marine Applications*, Texas, 245–262.

Hughes, J. M. O., Wroth, C. P. & Windle, D. (1977). Pressuremeter test in sands. *Géotechnique* **27,** 455–477.

Palmer, A. C. (1972). Undrained plane strain expansion of a cylindrical cavity in clays. *Géotechnique* **22,** 451–457.

Randolph, M. F., Carter, J. P. & Wroth, C. P. (1979). Driven piles in clay—the effects of installation and subsequent consolidation. *Géotechnique* **29,** 361–393.

Sagaseta, C. (1984). Quasi-static undrained expansion of a cylindrical cavity in clay in the presence of shaft friction and anistropic initial stresses. Personal communication.

Vesic, A. S. (1972). Expansion of cavities in infinite soil mass. *J. Soil Mech. Fndn Engng Div., Am. Soc. Civ. Engrs* **98,** 265–290.

Yu, H. S. (1990). *Cavity expansion theory and its application to the analysis of pressuremeters.* DPhil thesis, Oxford University, England.

Yu, H. S. & Houlsby, G. T. (1990). A new finite element formulation for one-dimensional analysis of elastic–plastic materials. *Computers and Geotechnics* **9**, No. 4, 241–256.

Yu, H. S. & Houlsby, G. T. (1991). Finite cavity expansion in dilatant soils: unloading analysis. *Géotechnique* (submitted).

Yu, H. S. & Houlsby, G. T. (1992). *Géotechnique* **42**, No. 4, 649–654

DISCUSSION

Finite cavity expansion in dilatant soils: loading analysis

H. S. YU and G. T. HOULSBY (1991). *Géotechnique* **41**, No. 2, 173–183

M. Manassero, *Ingegneria Geotecnica, Torino and Technical University of Torino*

The Paper presents innovative aspects of comparison of existing solutions to the problem of the expansion of cavities in soil. One of the most important features of the proposed approach seems to be the possibility of taking into account large strains and thus obtaining the complete stress–strain curve of the idealized material up to the limit cavity pressure p_∞ at infinite expansion.

Using the closed form solution of the Authors, it is interesting to compare the cylindrical cavity expansion stress–strain curve of the idealized soil with the experimental one obtained from self-boring pressuremeter tests (SBPT) carried out both in well-known natural sandy deposits and in a calibration chamber. The comparison can be carried out using the following steps.

(*a*) Plot the experimental curve from SBPTs using an appropriate coordinate $\Delta V/V$ for cavity strain, to allow complete and easy comparison with the theoretical functions from zero to infinite cavity expansion. Current volumetric cavity strain is given by

$$\Delta V/V = (V - V_0)/V$$

where V_0 is initial cavity volume and V is the current volume of the expanding cavity. For the cavity expansion coordinate used by the Authors

$$\Delta V/V = 1 - (a_0/a)^2 \tag{55}$$

(*b*) Extrapolate the SBPT curve to infinite cavity expansion using the method proposed by Ghionna, Jamiolkowski & Manassero (1990).

(*c*) Assess the plane strain peak friction angle ϕ_p of sandy material from cone penetration tests (CPT) (Jamiolkowski, Ghionna, Lancellotta & Pasqualini, 1988) and SBPTs (Manassero, 1989) for natural deposits and from laboratory triaxial tests (Baldi, Bellotti, Crippa, Fretti, Ghionna, Jamiolkowski, Morabito, Ostricati & Pasqualini, 1985) for calibration chamber specimens. Lade & Duncan's (1975) formula for calculating ϕ_p from the peak friction angle in axially symmetric strain conditions ϕ_{pt} gives

$$\phi_p{}^\circ = 1{\cdot}5\phi_{pt}{}^\circ - 17^\circ \tag{56}$$

(*d*) Assess the constant volume friction angle ($\phi_{cv} = 34°$) from ring shear tests on reconstituted samples (Baldi *et al.*, 1985; Carriglio, 1989).

(*e*) Assess the dilatancy angle ψ from ϕ_p and ϕ_{cv} using Rowe's (1972) formula

$$\frac{1 + \sin \phi_p}{1 - \sin \phi_p} = \frac{1 + \sin \phi_{cv}}{1 - \sin \phi_{cv}} \frac{1 + \sin \psi}{1 - \sin \psi} \tag{57}$$

which, in the range of interest, gives about the same results as Bolton's (1986) formula used by the Authors.

(*f*) Adopt a Poisson's ratio ν of 0·2.

(*g*) Assess shear modulus G imposing a limit cavity pressure from the Authors' method $p_{\infty YH}$ equal to the limit cavity pressure obtained using the extrapolation procedure of Ghionna *et al.*, $p_{\infty GJM}$.

The SBPTs were carried out

(*i*) in a calibration chamber test with a medium dense (relative density 65%) Ticino sand specimen (Ticino sand has been characterized by Baldi *et al.* (1985))

(*ii*) in a natural sandy deposit of the Po river with an estimated relative density of about 50–60% (Po river sand has been characterized by Bruzzi, Ghionna, Jamiolkowski, Lancellotta & Manfredini (1986)).

The first series of comparisons was performed using peak strength parameters and related values of G assessed by imposing $p_{\infty YH} = p_{\infty GJM}$. The second series used critical state strength parameters $\phi_p = \phi_{cv}$ (therefore $\psi = 0$) and related values of G from $p_{\infty YH} = p_{\infty GJM}$.

Two of the results obtained are shown in Fig. 11. Using the peak strength parameter for the idealized elastic perfectly plastic sand behaviour and given the G value to reach $p_{\infty GJM}$, there is a poor agreement with the experimental SBPT curve. Using the $\Delta V/V$ cavity strain coordinate, the continuously dilatant behaviour of the Authors' model gives a rather unusual shape to the last part of the curves in Figs 11(a) and 11(d) before reaching p_∞. This is probably due to the physical impossibility of the material being able to dilate to an infinite value. Good agreement is shown between the theoretical and experimental curves

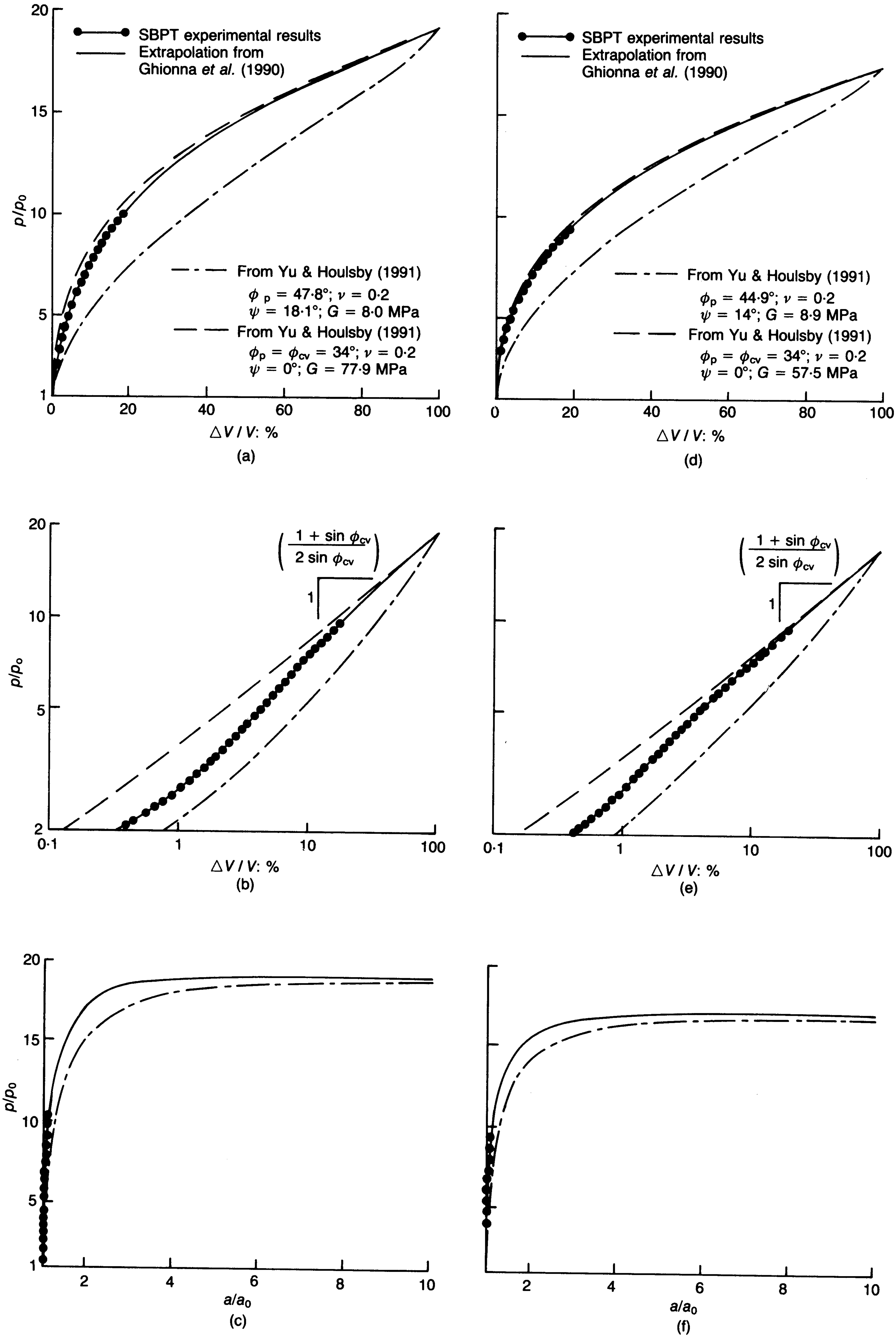

Fig. 11. Theoretical versus experimental cylindrical cavity expansion curves: (a), (b), (c) calibration chamber tests in Ticino sand; (d), (e), (f) in situ tests in Po river sand

using, for the elasto-plastic sand model, the critical state strength parameters $\phi_p = \phi_{cv}$ and $\psi = 0$ and G from $p_{\infty YH} = p_{\infty GJM}$. With these parameters the Authors' model and extrapolation procedure of Ghionna *et al.* (1990) give practically the same stress–strain relationships when the sandy element at the cavity wall reaches critical state conditions (Figs 11(b) and 11(e)).

These comments may be confirmed by plotting the theoretical and experimental curves using the strain coordinates of the Authors (Figs 11(c) and 11(f)).

The values of G/G_0 are plotted against relative density in Fig. 12 for a number of calibration chamber tests in Ticino sand, G_0 being the initial tangent shear modulus from resonant column tests (the reference deformability parameter for a given relative density and octahedral normal stress σ_0) and G the shear modulus from $p_{\infty YH} = p_{\infty GJM}$ using either peak or critical state strength parameters. Figure 12 shows that, using peak strength parameters, G/G_0 approaches a more or less constant value independent of the relative density of the calibration chamber specimen. However, as expected considering the unique value of $\phi_p = \phi_{cv} = 34°$, the ratio G/G_0 increases with increasing relative density.

Figure 12 can be useful in the assessment of deformability parameters of elastic perfectly plastic models when the limit pressure of cylindrical cavity expansion in cohesionless soils is to be estimated using the Authors' method.

Considering the limit pressure of cavities from available closed form solutions, it is interesting to compare the results of the Authors' and Carter, Booker & Yeung's (1986) procedures. Using the same strength and deformation parameters, in the range of interest for sandy soils, the solutions of the Author's and Carter *et al.* give very close results with a maximum variation of 1–2%.

A direct comparison of the Vésic (1972) solution with the other two procedures is not possible because of different input parameters. Vésic's formula needs constant volumetric deformation in the plastic zone ε_{vcv} instead of the dilation angle ψ used by the Authors' and Carter *et al.*

With regard to the actual behaviour of sands (Lade, 1972; Schofield & Wroth, 1968), in particular at large deformations, it seems more appropriate to consider constant volumetric strains rather than a constant angle of dilation in the assessment of limit cavity pressures.

As far as the range of shear strain smaller than 10% is concerned, taking as an example the SBPT in Po river sand, the best fit of Fig. 11(e) ($\phi_p = \phi_{cv} = 34°$ and $G = 57\,500$ kPa) significantly underpredicts cavity strain below $\Delta V/V = 10\%$ (i.e. shear strain at the cavity wall of about 10%). A much better fit can be obtained using peak strength and $G = 19\,500$ kPa, as shown in Fig. 13.

Due to SBPT equipment reliability at shear strain lower than $10^{-1}\%$, an effective comparison between experimental and theoretical results in the very small strain range is practically impossible.

It therefore seems that with a simple elastic perfectly plastic model it is very difficult to fit the complete real stress–strain behaviour of sandy soils satisfactorily (Fig. 14) and simple boundary problems like cylindrical cavity expansion. An alternative solution, without increasing the complexity of the mathematics or using numerical procedures, would be to split up the problem by referring to restricted ranges of the actual stress–

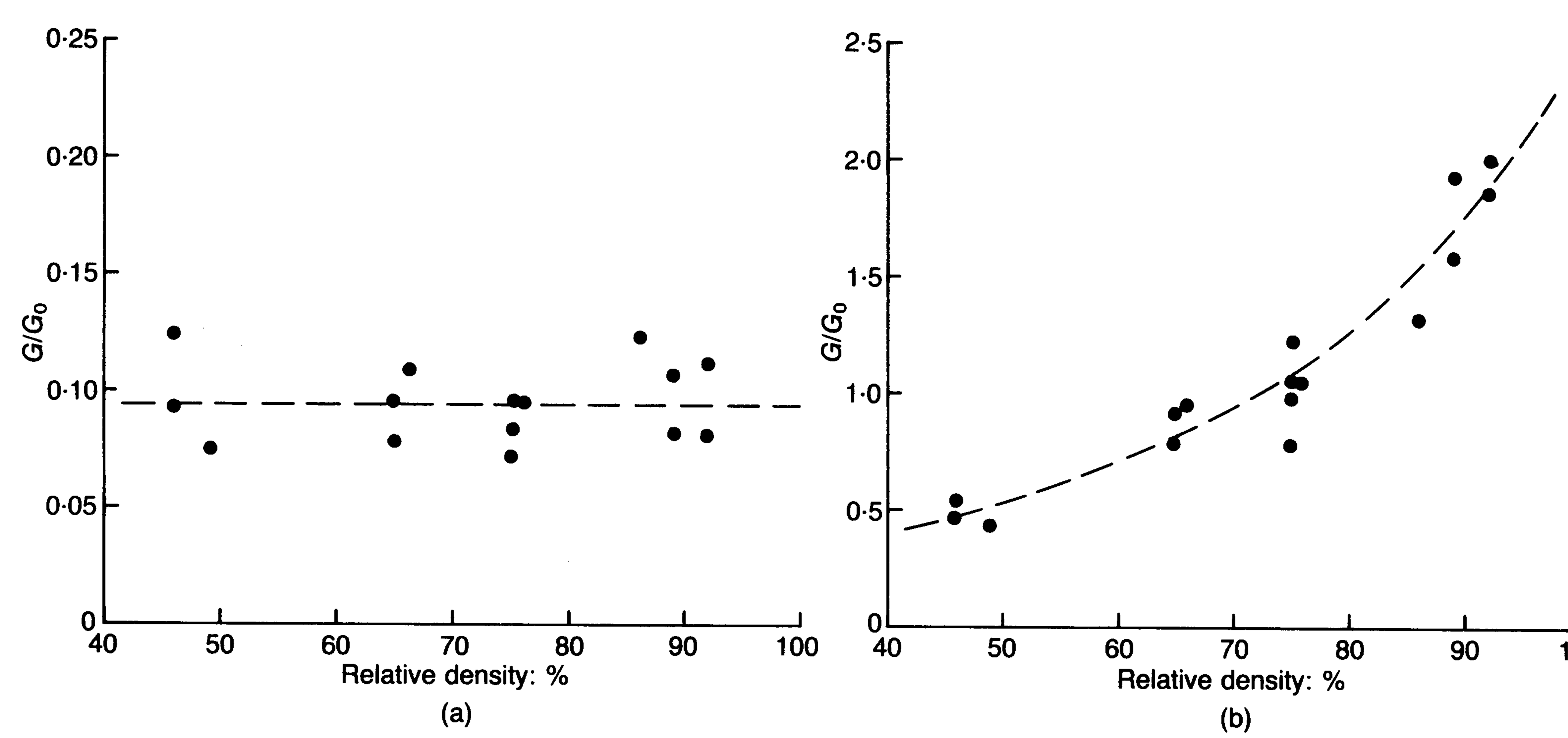

Fig. 12. Shear moduli ratio plotted against relative density (Ticino sand): (a) peak strength parameters; (b) critical state strength parameters

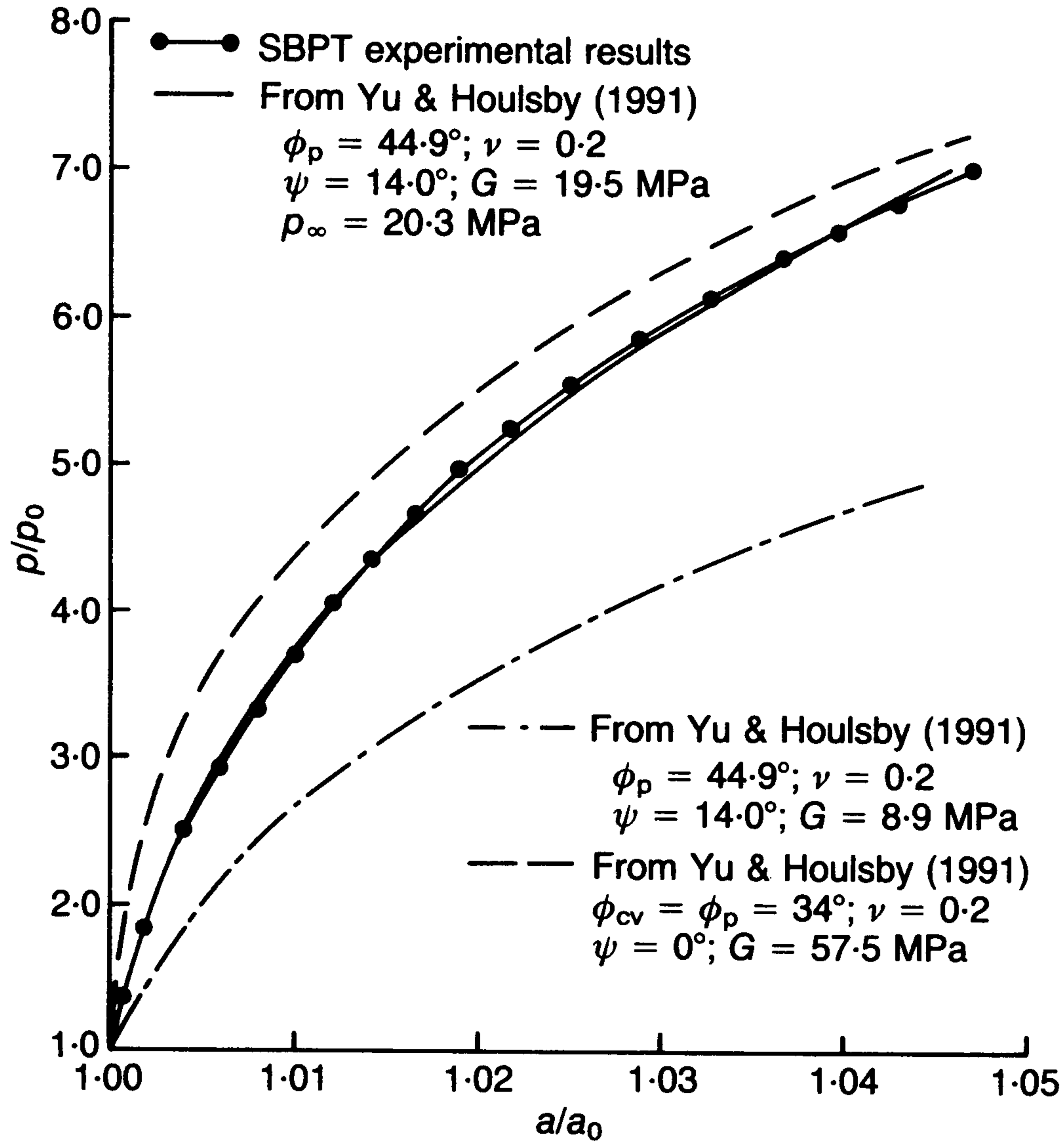

Fig. 13. Theoretical and experimental cylindrical cavity expansion curves at small strains

strain behaviour and to adopt the appropriate parameters, possibly those from back-analyses of experimental results.

Authors' reply

The Authors' analysis is applicable only to the case of an infinitely distant outer boundary, and therefore should be used only with great caution for the analysis of calibration chamber results. The influence of the proximity of the chamber boundary can be important, especially in cases where the zone of plastically deforming soil extends as far as the boundary (Schnaid & Houlsby, 1991).

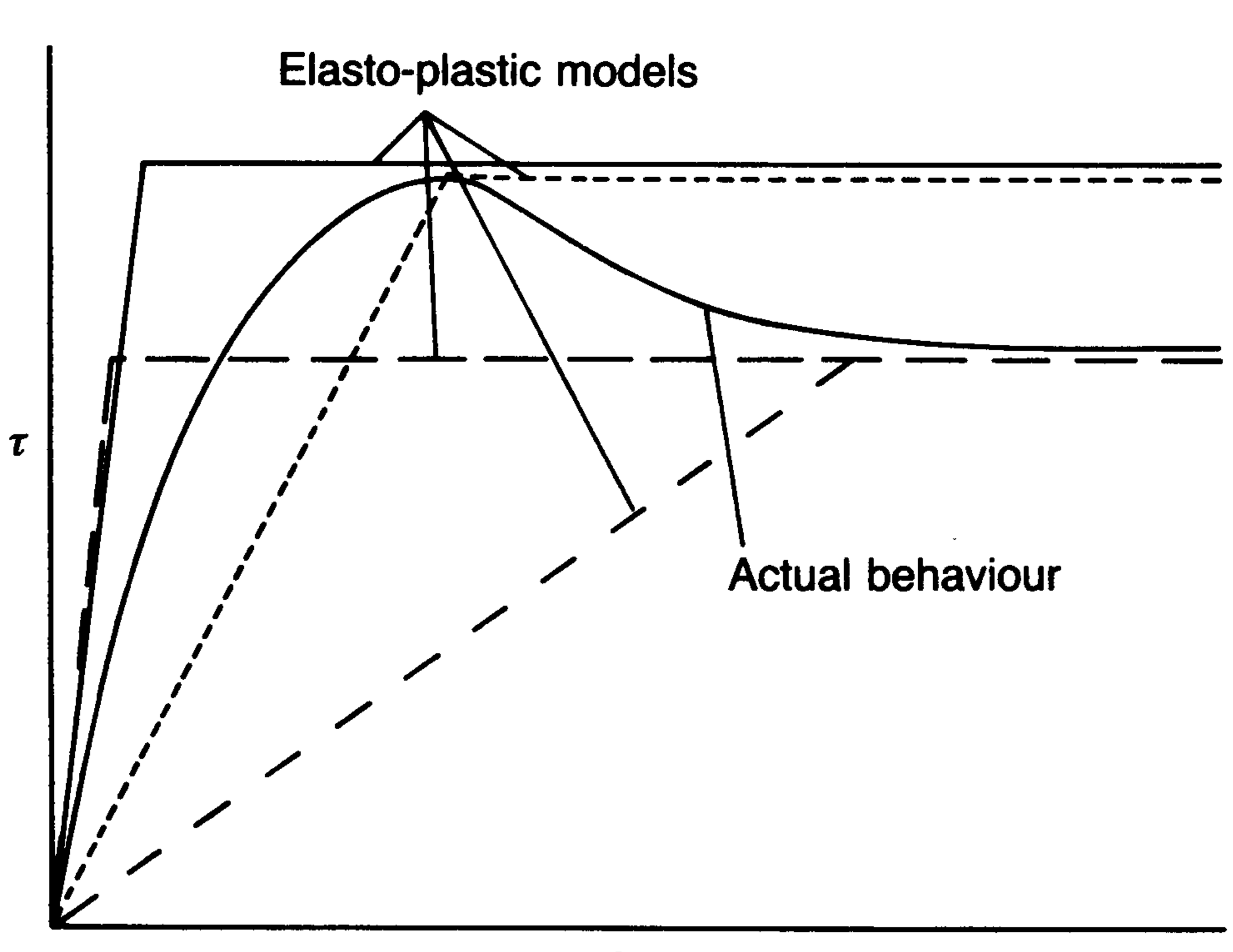

Fig. 14. Actual behaviour of sands and possible elastic-perfectly plastic models

Since the self-boring pressuremeter imposes only small strain, the extrapolation to obtain a limit pressure using, for instance, the procedure of Ghionna *et al.* (1990) is rather unreliable. The decision to match limit pressures from the Ghionna *et al.* and the Authors' analyses does not therefore seem to be justifiable. The matching was used to determine the appropriate shear modulus, which can be determined much better from unload–reload loops.

The result of matching the limit pressures in this way is that in, for instance, Fig. 11(a) the shear modulus used in conjunction with the peak friction angle is only one tenth of the value of that used in conjunction with the critical state value. If a reasonable estimate of the shear modulus were to be made from unload–reload loops, then a more rational comparison of different friction angles could be made using the same modulus in each case (but implying different limit pressures).

Manassero chooses the strain axis $\Delta V/V$ for convenience, because at large strain this measure approaches unity. This has the effect of compressing the higher values of the more usual stress–strain curve plotted in terms of linear strain. The unusual shape of the curves predicted by the Author is due entirely to Manassero's choice of an unusual strain measure, and is unrelated to the dilation implied by the model. This is shown, for instance, by the curves in Fig. 11(c).

Bearing in mind these concerns about matching of the limit pressure, it is not surprising that when using peak strength values a rather low G/G_0 value is determined (Fig. 12(a)), nor that much higher (and inconsistent) values are needed in conjunction with critical state strengths (Fig. 12(b)). As the density is increased, the critical state strength becomes an increasingly bad underestimate of the relevant strength, so that to achieve the same limit pressure an increasingly unrealistic overestimate of G/G_0 must be used. For dense sands this implies an unacceptable value of G/G_0 greater than 1·0, but this is due entirely to the choice of matching the limit pressures from two analyses.

It is reassuring to see (Fig. 13) that a realistic choice of shear modulus and strength parameters results in a very close fitting of the observed curve by the Authors' analysis.

Corrigendum

In the Paper there is an inconsistency between the algebra and Figs 7–10. The algebra is correct and the figures are in error. Corrected versions of Figs 7–10 are presented here. The result is a slight reduction of limit pressure in cases where $\psi \neq 0$. The consequential changes to the text are

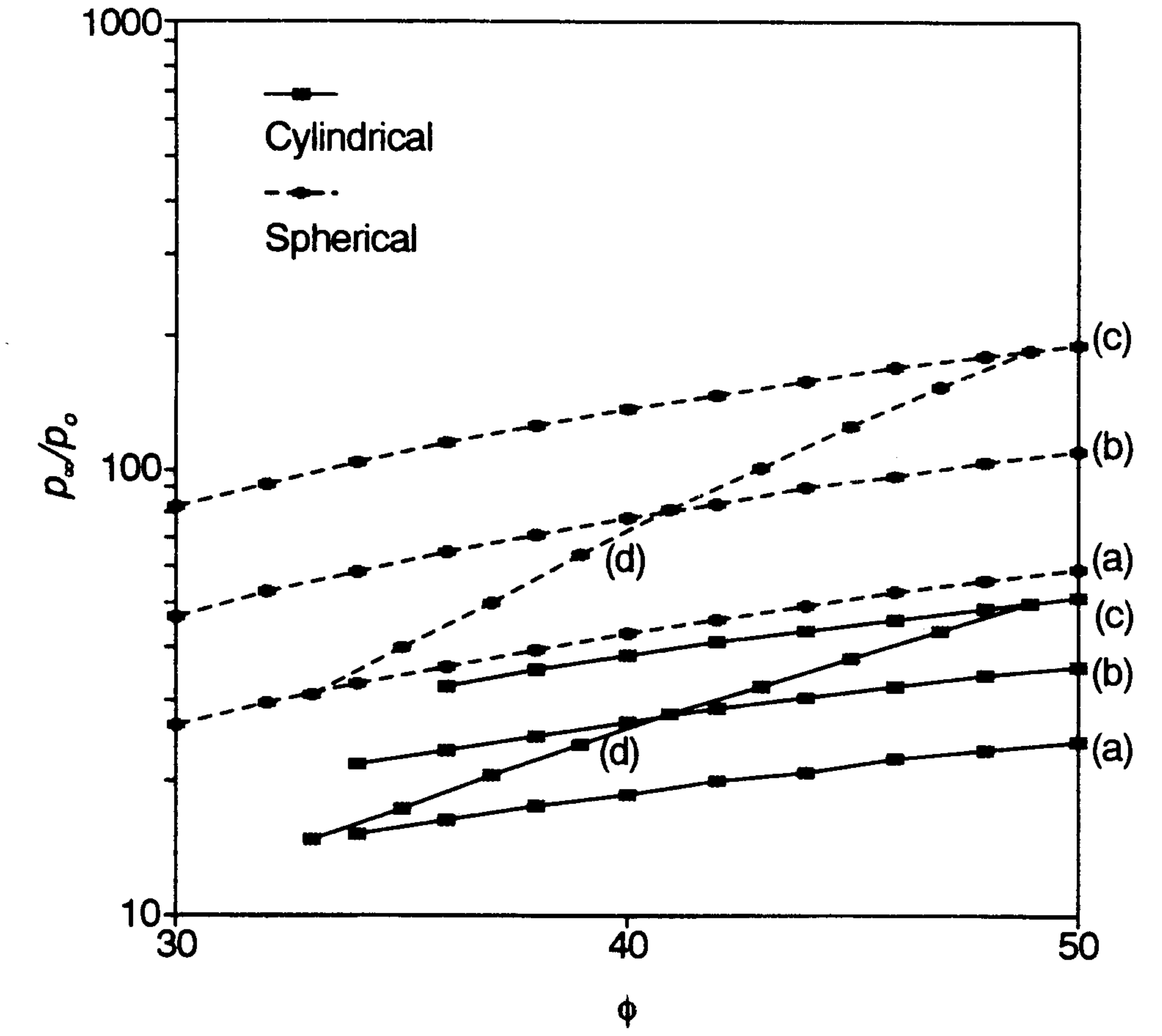

Fig. 7. Variation of limit pressure with angle of friction, $G/p_0 = 500$, $\nu = 0{\cdot}2$: (a) $\psi = 0°$; (b) $\psi = 10°$; (c) $\psi = 20°$; (d) $\phi = 33° + 0{\cdot}8\psi$

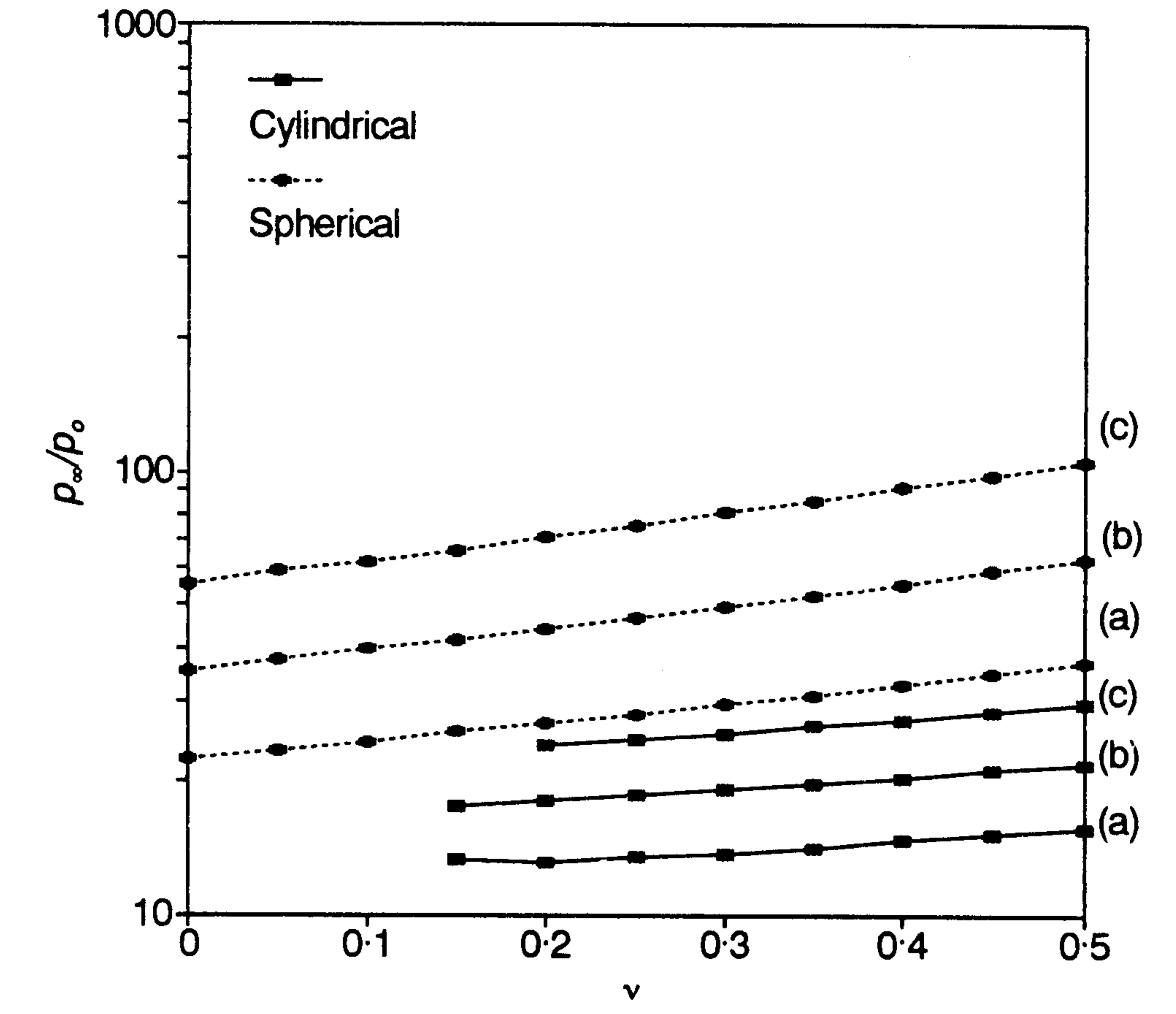

Fig. 9. Variation of limit pressure with Poisson's ratio, $G/p_0 = 200$, $\psi = 40°$: (a) $\psi = 0°$; (b) $\psi = 10°$; (c) $\psi = 20°$

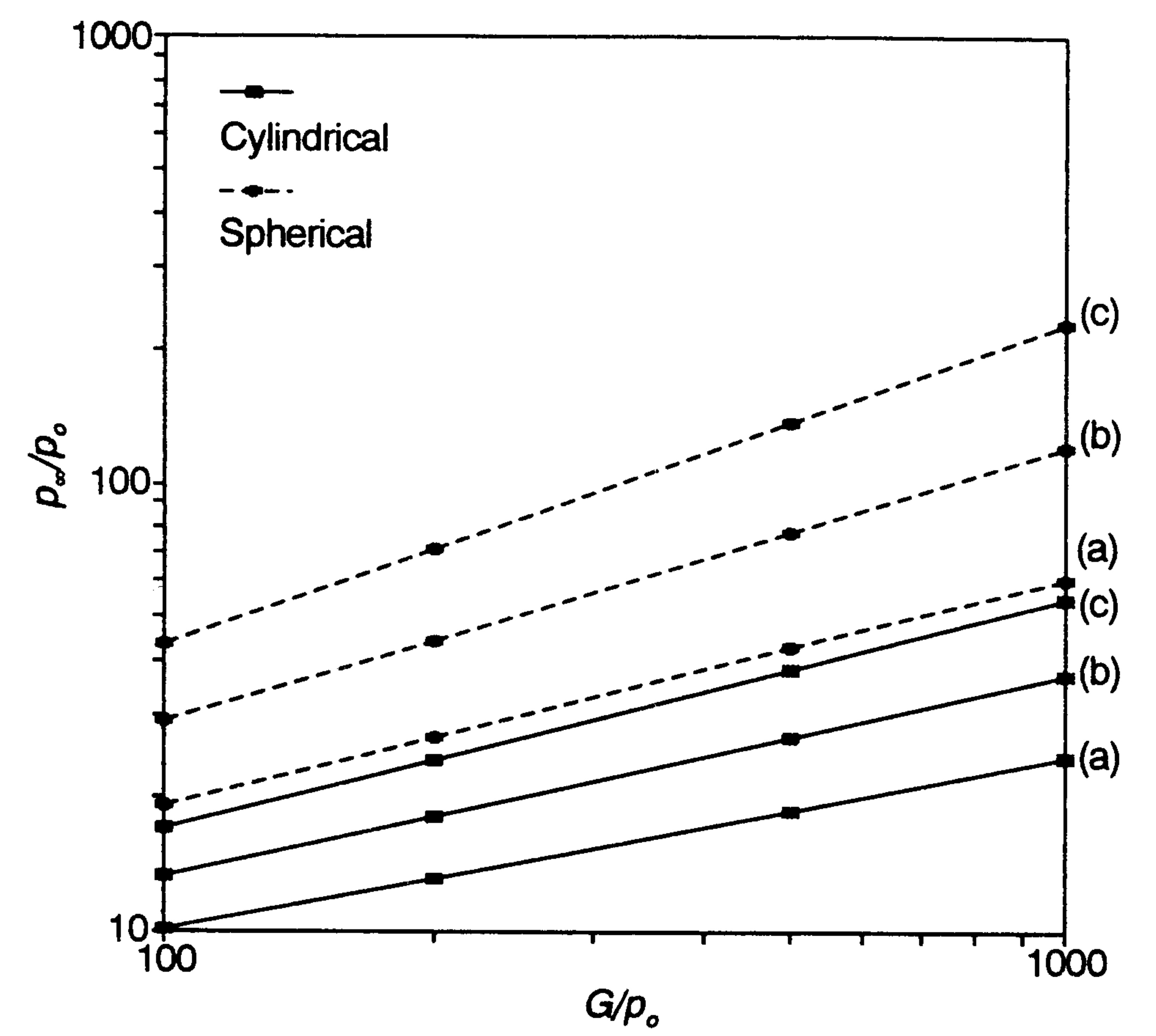

Fig. 8. Variation of limit pressure with stiffness, $\nu = 0{\cdot}2$, $\phi = 40°$: (a) $\phi = 0°$; (b) $\phi = 10°$; (c) $\phi = 20°$

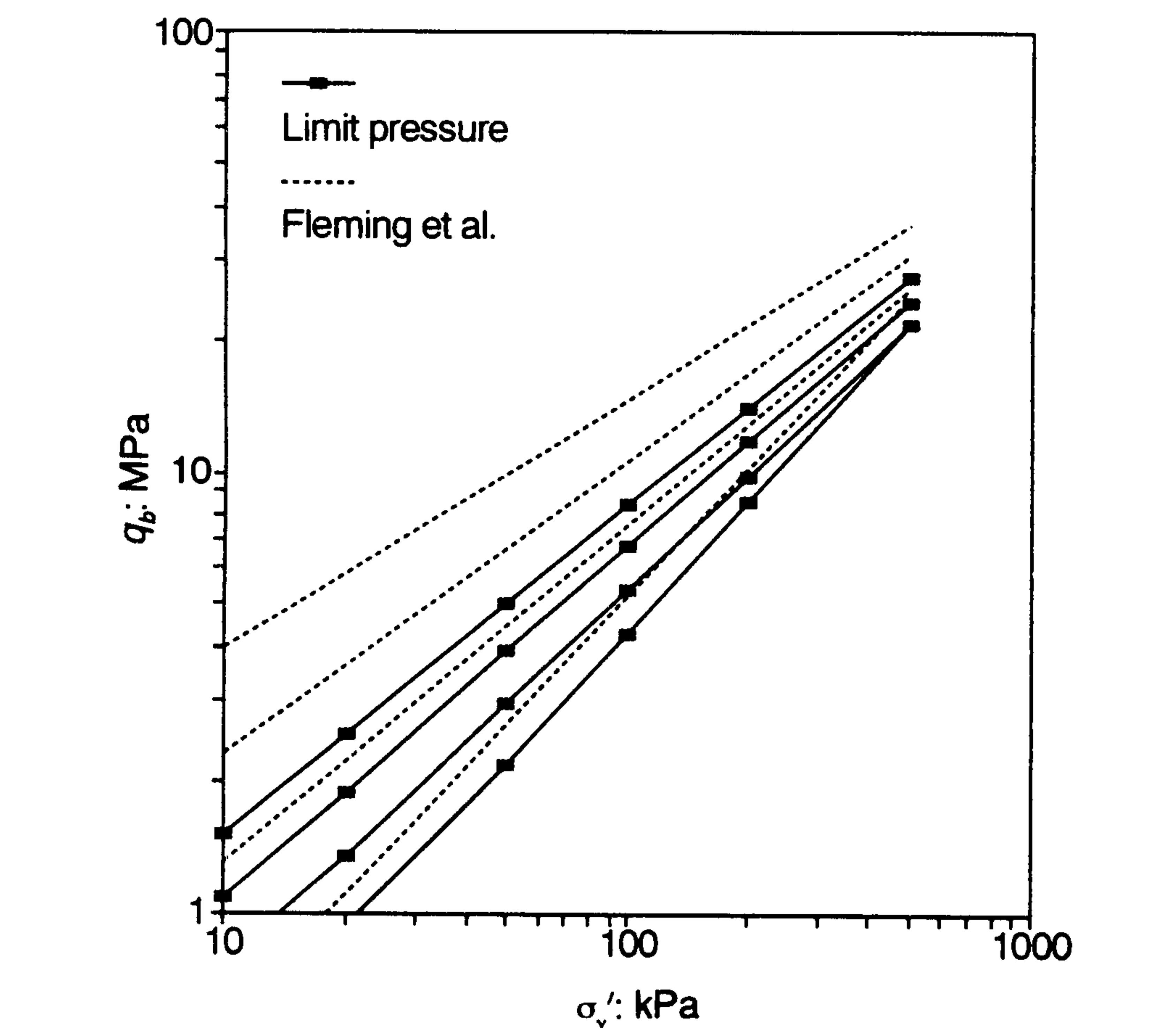

Fig. 10. End bearing capacity of piles calculated by limit pressure method, compared to chart given by Fleming *et al.* (1985), $\phi_{cv} = 33°$

(*a*) referring to Fig. 7, the limit pressure is 184 p_0 at $\phi = 49°$

(*b*) referring to Fig. 10, the cavity expansion solution is lower than the Fleming *et al.* (1985) solution by a factor of between 0·8 for loose sand and 0·4 for dense sand; these figures still depend on the choice of G/p_0 value.

REFERENCES

Baldi, G., Bellotti, R., Crippa, V., Fretti, C., Ghionna, V. N., Jamiolkowski, M., Morabito, P., Ostricati, D. & Pasqualini, E. (1985). Laboratory validation of in situ tests. *Proc. 11th Int. Conf. Soil Mech., San Francisco*, 251–270.

Bolton, M. D. (1986). The strength and dilatancy of sands. *Géotechnique* **36,** No. 1, 65–78.

Bruzzi, D., Ghionna, V. N., Jamiolkowski, M., Lancellotta, R & Manfredini, G. (986). Self-boring pressuremeter in Po river sand. *Proc. 2nd Int. Symp. Pressuremeter Marine Applications, Texas*, STP 950, 57–73. Austin: American Society for Testing and Materials.

Carriglio, F. (1989). *Mechanical behaviour of sands.* DPhil Thesis, Technical University of Turin.

Carter, J. P., Booker, J. R. & Yeung, S. K. (1986). Cavity expansion in cohesive frictional soils. *Géotechnique* **36**, No. 3, 349–353.

Ghionna, V. N., Jamiolkowski, M. & Manassero, M. (1990). Limit pressure in expansion of cylindrical cavity in sand. In *Pressuremeters*, London: Thomas

Telford, 149–158.

Jamiolkowski, M., Ghionna, V. N., Lancellotta, R. & Pasqualini, E. (1988). New correlations of penetration tests for design practice. *Proceedings of ISOPT, Orlando*, 263–296.

Lade, P. V. (1972). *The stress–strain and strength characteristics of cohesionless soils.* PhD thesis, University of California.

Lade, P. V. & Duncan, J. M. (1975). Elastoplastic stress–strain theory for cohesionless soil. *J. Geotech. Engng Div. Am. Soc. Civ. Engrs* **101,** GT 10, 1037–1053.

Manassero, M. (1989). Stress–strain relationships from drained self-boring pressuremeter test in sands. *Géotechnique* **39,** No. 2, 293–307.

Rowe, P. W. (1972). Stress–strain relationship for particulate materials at equilibrium. *Proceedings of the specialty conference on the performance of earth-supported structures.* New York: American Society of Civil Engineers, 327–359.

Schofield, A. N. & Wroth, C. P. (1968). *Critical state soil mechanics*. London: McGraw-Hill.

Schnaid, F. & Houlsby, G. T. (1991). An assessment of chamber size effects in the calibration of in situ tests in sand. *Géotechnique* **41,** No. 3, 437–445.

Vésic, A. S. (1972). Expansion of cavities in infinite soil mass. *J. Soil Mech. Fdns Div. Am. Soc. Civ. Engrs* **98,** SM 3, 265–290.